Recounting the FANTOM Cage Associated Transcriptome

Eddie-Luidy Imada[1,2,+], Diego Fernando Sanchez[1,+], Leonardo Collado-Torres[3], Christopher Wilks[4], Tejasvi Matam[1], Wikum Dinalankara[1], Aleksey Stupnikov[1], Francisco Lobo-Pereira[5], Chi-Wai Yip[6], Kayoko Yasuzawa[6], Naoto Kondo[6], Masayoshi Itoh[7], Harukazu Suzuki[6], Takeya Kasukawa[6], Chung Chau Hon[6], Michiel de Hoon[6], Jay W Shin[6], Piero Carninci[6], FANTOM consortium , Andrew E Jaffe[3,8,9], Jeffrey T Leek[9], Alexander Favorov[1,10], Gloria R Franco[2], Ben Langmead[4,9,*], and Luigi Marchionni[1,*,+,a]

[1]Department of Oncology, Johns Hopkins University School of Medicine, Baltimore, MD, USA
[2]Departamento de Bioquímica e Imunologia, ICB, Universidade Federal de Minas Gerais, Belo Horizonte, MG, Brazil
[3]Lieber Institute for Brain Development, Baltimore, MD, USA
[4]Department of Computer Science, Johns Hopkins University, Baltimore, MD, USA
[5]Departamento de Biologia General, ICB, Universidade Federal de Minas Gerais, Belo Horizonte, MG, Brazil
[6]RIKEN Center for Integrative Medical Sciences, Yokohama, Japan
[7]RIKEN, Preventive Medicine Diagnostic Innovation Program, Yokohama, Japan
[8]Department of Mental Health, Johns Hopkins Bloomberg School of Public Health, Baltimore, MD, USA
[9]Department of Biostatistics, Johns Hopkins Bloomberg School of Public Health, Baltimore, MD, USA
[10]Laboratory of Systems Biology and Computational Genetics, VIGG RAS, Moscow, RF
[*,+]These authors contributed equally to this work
[a]Correspondence to Luigi Marchionni (marchion@jhu.edu)

ABSTRACT

Long non-coding RNAs (lncRNAs) have emerged as key coordinators of biological and cellular processes. Characterizing lncRNA expression across cells and tissues is key to understanding their role in determining phenotypes including disease. We present here `FC-R2`, a comprehensive expression atlas across a broadly-defined human transcriptome, inclusive of over 100,000 coding and non-coding genes as described by the FANTOM CAGE-Associated Transcriptome (FANTOM-CAT) study. This atlas greatly extends the gene annotation used in the original *recount2* resource. We demonstrate the utility of the `FC-R2` atlas by reproducing key findings from published large studies and by generating new results across normal and diseased human samples. In particular, we (a) identify tissue specific transcription profiles for distinct classes of coding and non-coding genes, (b) perform differential expression analysis across thirteen cancer types, providing new insights linking promoter and enhancer lncRNAs expression to tumor pathogenesis, and (c) confirm the prognostic value of several enhancers in cancer. Comprised of over 70,000 samples, `FC-R2` will empower other researchers to investigate the roles of both known genes and recently described lncRNAs. Access to the `FC-R2` atlas is available from `https://jhubiostatistics.shinyapps.io/recount/`, the *recount* Bioconductor package, and `http://marchionnilab.org/fcr2.html`.

Introduction

Long non-coding RNAs (lncRNAs) are commonly defined as transcripts devoid of open reading frames (ORFs) longer than 200 nucleotides, which are often polyadenylated. This definition is not based on their function, since lncRNAs are involved in distinct molecular processes and biological contexts not yet fully characterized[1]. Over the past few years, the importance of lncRNAs has been clarified, leading to an increasing focus on decoding the consequences of their modulation and studying their involvement in the regulation of key biological mechanisms during development, normal tissue and cellular homeostasis, and in disease[1–3].

Given the emerging and previously underestimated importance of non-coding RNAs, the FANTOM consortium has initiated the systematic characterization of their biological function. Through the use of Cap Analysis of Gene Expression sequencing (CAGE-seq), combined with RNA-seq data from the public domain, the FANTOM consortium released a comprehensive atlas of the human transcriptome, encompassing more accurate transcriptional start sites (TSS) for coding and non-coding genes, including numerous novel long non-coding genes: the FANTOM CAGE Associated Transcriptome (*FANTOM-CAT*)[4]. We hypothesized that these lncRNAs can be measured in many RNA-seq datasets from the public domain and that they have been so far missed by the lack of a comprehensive gene annotation.

Although the systematic analysis of lncRNAs function is being addressed by the FANTOM consortium in loss of function studies, increasing the detection rate of these transcripts combining different studies is difficult because the heterogeneity of analytic methods employed. Current resources that apply uniform analytic methods to create expression summaries from public data do exist but can miss several lncRNAs because their dependency on a pre-existing gene annotation for creating the genes expression summaries[5,6]. We recently created *recount2*[7], a collection of uniformly-processed human RNA-seq data, wherein we summarized 4.4 trillion reads from over 70,000 human samples from the Sequence Reads Archive (SRA), The Cancer Genome Atlas (TCGA)[8], and the Genotype-Tissue Expression (GTEx)[9] projects[7]. Importantly, *recount2* provides annotation-agnostic coverage files that allow re-quantification using a new annotation without having to re-process the RNA-seq data.

Given the unique opportunity to access lastest results to the most comprehensive human transcriptome (the *FANTOM-CAT*project) and the *recount2* gene agnostic summaries, we addressed the previous described challenges building a comprehensive atlas of coding and non-coding gene expression across the human genome: the *FANTOM-CAT/recount2* expression atlas (`FC-R2` hereafter). Our resource contains expression profiles for 109,873 putative genes across over 70,000 samples, enabling an unparalleled resource for the analysis of the human coding and non-coding transcriptome.

Results

Building the *FANTOM-CAT/recount2* resource

The *recount2* resource includes a coverage track, in the form of a BigWig file, for each processed sample. We built the `FC-R2` expression atlas by extracting expression levels from *recount2* coverage tracks in regions that overlapped unambiguous

exon coordinates for the permissive set of *FANTOM-CAT* transcripts, according to the pipeline shown in Figure 1. Since *recount2*'s coverage tracks does not distinguish from between genomic strands, we removed ambiguous segments that presented overlapping exon annotations from both strands (see Methods section). After such disambiguation procedure, the remaining 1,066,515 exonic segments mapped back to 109,869 genes in *FANTOM-CAT* (out of the 124,047 starting ones included in the permissive set[4]). Overall, the `FC-R2` expression atlas encompasses 2,041 studies with 71,045 RNA-seq samples, providing expression information for 22,116 coding genes and 87,763 non-coding genes, such as enhancers, promoters, and others lncRNAs.

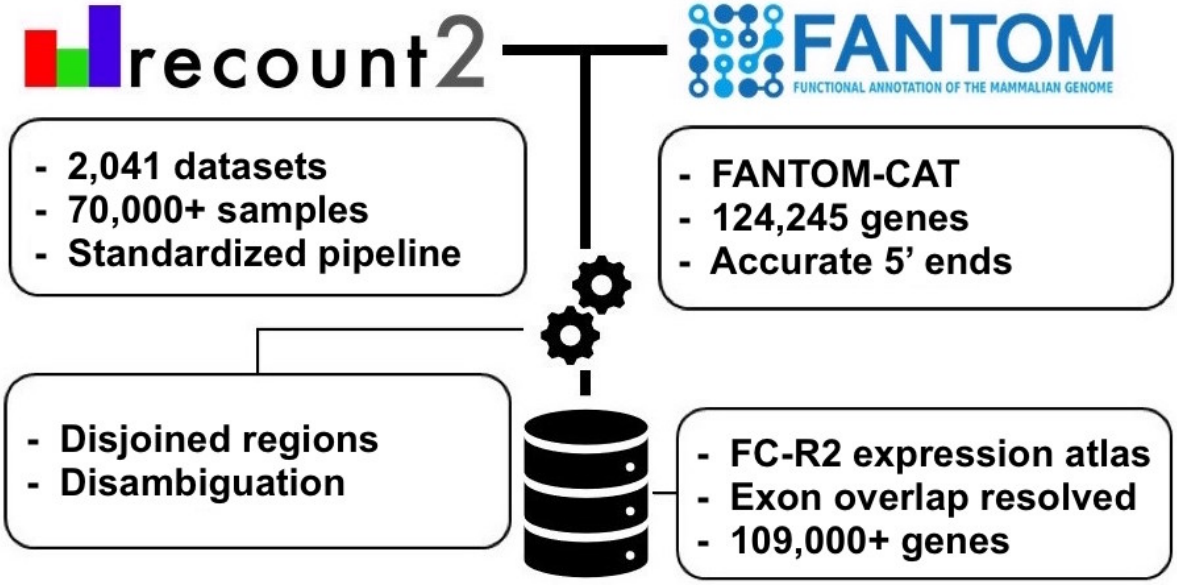

Figure 1. Overview of the *FANTOM-CAT/recount2* resource development. `FC-R2` leverages two public resources, the *FANTOM-CAT* gene models and *recount2*. `FC-R2` provides expression information for 109,873 genes, both coding (22,110) and non-coding (87,693). This latter group encompasses enhancers, promoters, and others lncRNAs.

Validating the *FANTOM-CAT/recount2* resource

We first assessed how gene expression estimates in `FC-R2` compared to previous gene expression estimates from other projects. Specifically, we considered data from the GTEx consortium (v6), spanning 9,662 samples from 551 individuals and 54 tissues types[9]. First, we correlated gene expression levels between the `FC-R2` atlas and quantification based on GENCODE (v25) in *recount2* for the GTEx data, observing a median correlation ≥ 0.986 for the 32,922 genes in common. This result supports the notion that our pre-processing steps to disambiguate overlapping exon regions between strands did not significantly alter gene expression quantification.

Next, we assesed whether gene expression specificity, as measured in `FC-R2`, was maintained across tissue types. To this end, we selected and compared gene expression for known tissue-specific expression patterns, such as Keratin 1 (*KRT1*), Estrogen Receptor 1 (*ESR1*), and Neuronal Differentiation 1 (*NEUROD1*) (Figure 2). Overall, all analyzed tissue specific markers presented nearly identical expression profiles across GTEx tissue types between the alternative gene models considered

(see Figure 2 and S1), confirming the consistency between gene expression quantification in `FC-R2` and those based on GENCODE.

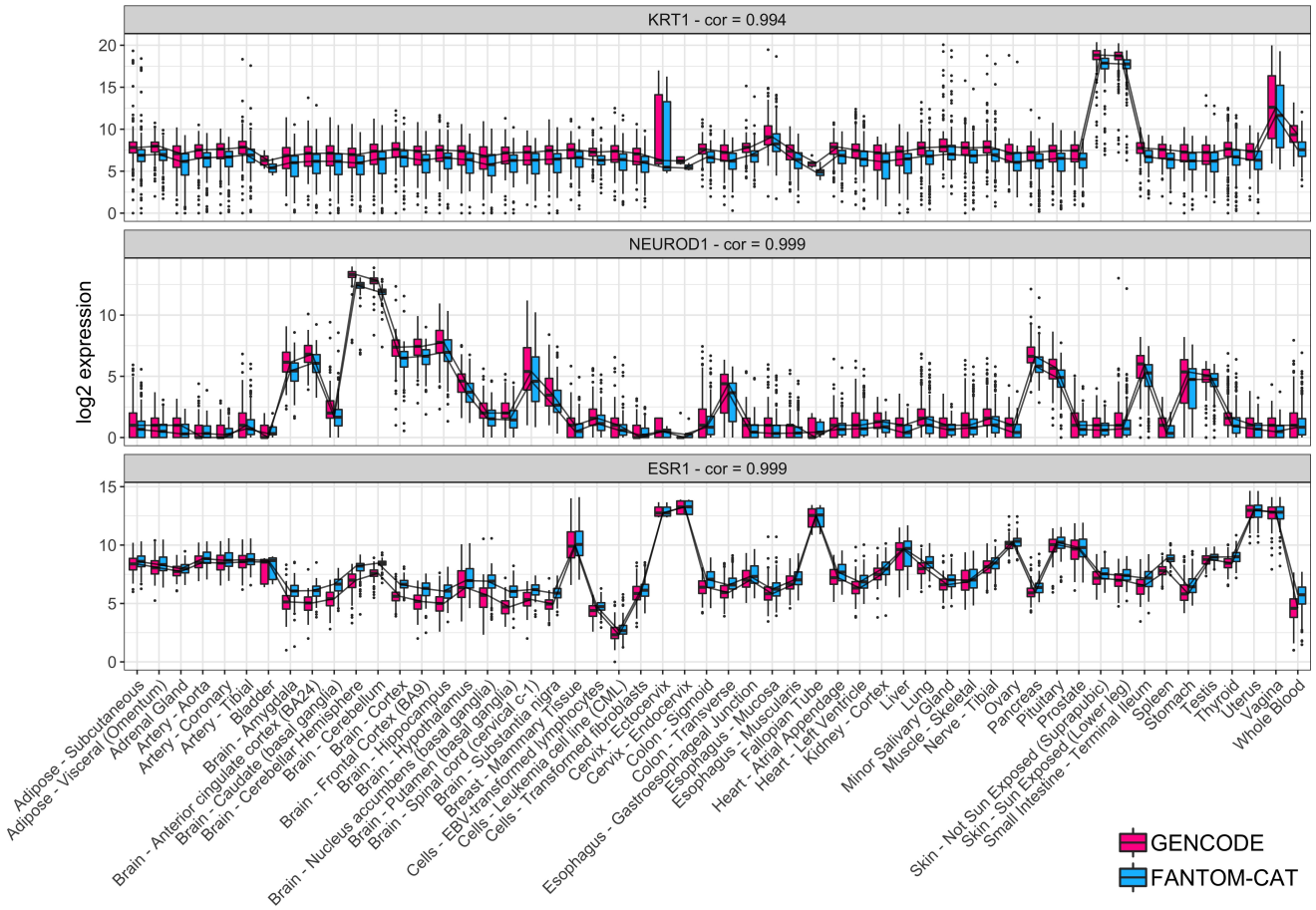

Figure 2. Tissue specific expression in GTEx. Log2 expression for three tissue specific genes (*KRT1*, *NEUROD1*, and *ESR1*) in GTEx data stratify by tissue type using `FC-R2` and GENCODE based quantification. Expression profiles are highly correlated and expressed consistently in the expected tissue types (*e.g.*, *KRT1* is most expressed in skin, *NEUROD1* in brain, and *ESR1* in estrogen sensitive tissue types like uterus, Fallopian tubes, and breast). Correlations are shown on top for each tissue marker. Center lines, upper/lower quartiles and Whiskers represents the median, 25/75 quartiles and 1.5 interquartile range, recpectively.

Tissue-specific expression of lncRNAs

It has been shown that, although expressed at a lower level, enhancers and promoters are not ubiquitously expressed and are more specific for different cell types than coding genes[4]. In order to verify this finding, we used GTEx data to assess expression levels and specificity profiles across samples from each of the 54 analyzed tissue types, stratified into four distinct gene categories: coding mRNA, intergenic promoter lncRNA (ip-lncRNA), divergent promoter lncRNA (dp-lncRNA), and enhancers lncRNA (e-lncRNA). Overall, we were able to confirm that these RNA classes are expressed at different levels, and that they display distinct specificity patterns across tissues, as shown for primary cell types by Hon et al.[4], albeit with more variability likely due to the increased cellular complexity present in tissues. Specifically, coding mRNAs were expressed at higher levels

than lncRNAs (log2 median expression of 6.6 for coding mRNAs, and of 4.1, 3.8 and 3.1, for ip-lncRNA, dp-lncRNA, and e-lncRNA, respectively). In contrast, the expression of enhancers and intergenic promoters was more tissue-specific (median = 0.41 and 0.30) than what observed for divergent promoters and coding mRNAs (median = 0.13 and 0.09) (Figure 3). Finally, when analyzing the percentage of genes expressed across tissues by category, we observed that coding genes are, in general, ubiquitous, while lncRNAs are more specific, with enhancers showing the lowest percentages of expressed (mean ranging from 88.42% to 41.98%, see Figure 3B), in agreement with the notion that enhancer transcription is tissue specific[10].

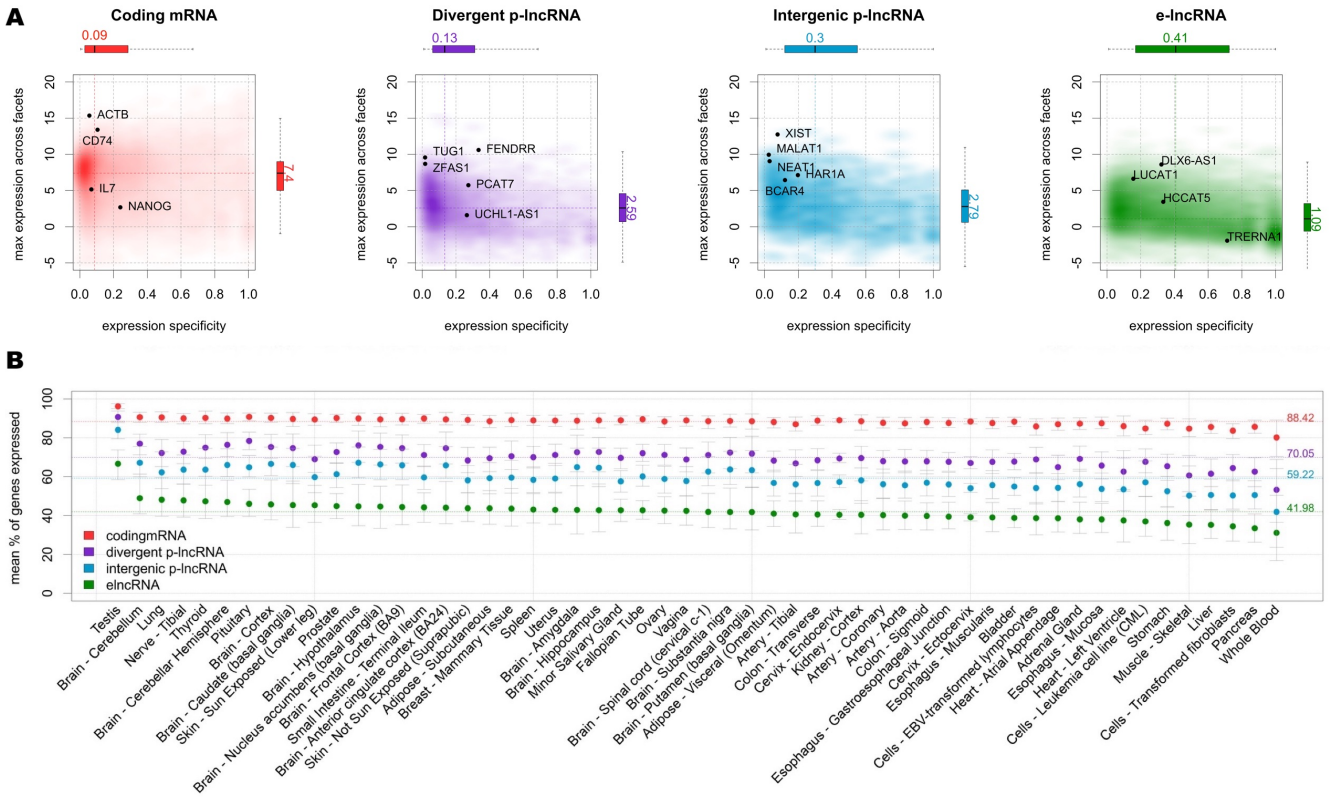

Figure 3. Expression profiles across GTEx tissues. A) Expression level and tissue specificity across four distinct RNA categories. The Y-axis shows log2 expression levels representing each gene using its maximum expression in GTEx tissues expressed as transcripts per million (TMP). The X-axis shows expression specificity based on entropy computed from median expression of each gene across the GTEx tissue types. Individual genes are highlighted in the figure panels. **B)** Percentage of genes expressed for each RNA category stratified by GTEx tissue facets. The dots represent the mean among samples within a facet and the error bars represent 99.99% confidence intervals. Dashed lines represent the means among all samples.

Differential expression analysis of coding and non-coding genes in cancer

We analyzed coding and non-coding gene expression in cancer using TCGA data. To this end, we compared cancer to normal samples separately for 13 tumor types, using `FC-R2` re-quantified data. We further identified the differentially expressed genes (DEG) in common across the distinct cancer types (see Figure 4). Overall, the number of DEG varied across cancer types and by gene class, with a higher number of significant coding than non-coding genes (FDR < 0.01, see table 1). Importantly, a substantial fraction of these genes was exclusively annotated in the *FANTOM-CAT*, suggesting that relying on other gene

models would result in missing many potential important genes (see Table 1). We then analyzed the consensus among cancer types. A total of 41 coding mRNAs were differentially expressed across all the 13 tumor types after global correction for multiple testing (FDR $< 10^{-6}$, see Supplementary table S1). For lncRNAs, a total of 28 divergent promoters, 4 intergenic promoters, and 3 enhancers were consistently up- or down-regulated across all the 13 tumor types after global correction for multiple testing (FDR < 0.1, see Supplementary tables S2, S3, S4, respectively).

Table 1. Differentially expressed genes in cancer. The table below summarizes the number of significant DEG ($FDR \leq 0.01$) between tumor and normal samples across the 13 cancer types analyzed for each gene class considered (coding mRNA, ip-lncRNA, dp-lncRNA, and e-lncRNA). Counts are reported separately for DEG up- and down-regulated in cancer, and values in parenthesis represents the number of genes exclusively annotated in the *FANTOM-CAT* gene model. Mean and standard deviation across cancer types is shown at the bottom.

		dp-lncRNA		e-lncRNA		ip-lncRNA		mRNA	
Cancer type	Total	Up	Down	Up	Down	Up	Down	Up	Down
Bile	7010	200 (60)	313 (90)	186 (89)	203 (99)	47 (12)	84 (17)	2658 (106)	3319 (97)
Bladder	7680	344 (125)	319 (87)	140 (68)	149 (67)	65 (19)	82 (7)	3112 (201)	3469 (61)
Breast	15290	753 (291)	721 (202)	656 (377)	583 (305)	207 (50)	178 (32)	6109 (296)	6083 (244)
Colorectal	13685	490 (164)	592 (168)	381 (203)	400 (196)	130 (32)	160 (28)	5538 (371)	5994 (132)
Esophagus	4883	87 (21)	193 (50)	90 (38)	184 (103)	40 (11)	48 (2)	1921 (83)	2320 (77)
Head and Neck	10517	442 (138)	401 (96)	267 (139)	251 (112)	100 (23)	109 (18)	4329 (256)	4618 (53)
Kidney	15697	734 (238)	820 (281)	535 (299)	486 (209)	203 (45)	200 (48)	6349 (525)	6370 (114)
Liver	10554	346 (94)	395 (106)	230 (102)	248 (123)	90 (16)	112 (19)	4164 (174)	4969 (95)
Lung	17143	864 (338)	835 (304)	893 (512)	729 (396)	242 (76)	213 (39)	7523 (532)	5844 (212)
Prostate	13183	686 (287)	654 (218)	418 (254)	452 (214)	175 (55)	167 (30)	5153 (489)	5478 (128)
Stomach	11309	528 (213)	518 (164)	462 (291)	436 (240)	144 (51)	129 (22)	4509 (558)	4583 (89)
Thyroid	14264	752 (284)	804 (318)	527 (295)	594 (332)	161 (39)	174 (47)	5403 (189)	5849 (308)
Uterus	12906	641 (285)	713 (235)	454 (263)	612 (341)	210 (79)	225 (54)	5135 (335)	4916 (181)
Mean	11855	528 (195)	560 (178)	403 (225)	410 (211)	140 (39)	145 (28)	4762 (317)	4909 (138)
St. Dev	3650	237 (102)	218 (89)	225 (137)	189 (107)	67 (23)	55 (16)	1557 (167)	1234 (77)

Next, we reviewed the literature to assess functional correlates for these consensus genes. Most of the consensus up-regulated coding genes (Supplementary Table S1) participate in cell cycle regulation, cell division, DNA replication and repair, and chromosome segregation, and mitotic spindle checkpoints. Most of the consensus down-regulated mRNAs (Supplementary Table S1) are associated with metabolism and oxidative stress, transcriptional regulation, cell migration and adhesion, and with modulation of of DNA damage repair and apoptosis.

Down-regulated dp-lncRNAs were mostly those associated with immune cells (*e.g.*, natural killer cells, T cell, and mature B-cells). Three genes, *RP11-276H19*, *RPL34-AS1*, and *RAP2C-AS1*, were reported to be implicated in cancer (Supplementary Table S2). The first controls epithelial-mesenchymal transition, the second is associated with tumor size increase, and the

third is associated with urothelial cancer after kidney cancer transplantation[11–13]. Among up-regulated dp-lncRNA, *SNHG1* (Supplementary Table S2) was implicated in cellular proliferation, migration, invasion of different cancer types, and strongly up-regulated in osteosarcoma, non-small lung cancer, and gastric cancer[14,15].

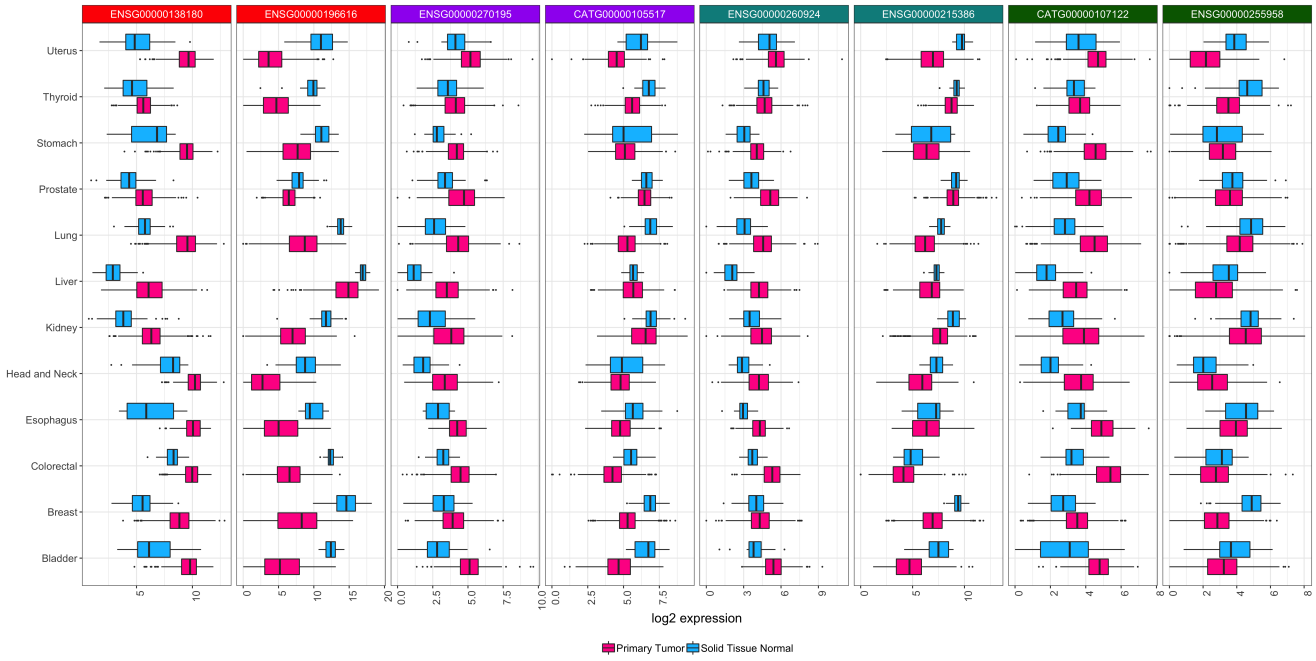

Figure 4. Differential expression for selected transcripts from distinct RNA classes across tumor types. Boxplots showing raw expression levels of differential expressed genes between tumor and normal tissue samples for all 13 tumor types analyzed. For each tissue of origin, the most up-regulated (on the left) and down-regulated (on the right) gene for each RNA class is shown. Center lines, upper/lower quartiles and Whiskers represents the median, 25/75 quartiles and 1.5 interquartile range, recpectively. Color coding on top of the figure indicates the RNA class (red for mRNA, purple for dp-lncRNA, cyan ip-lncRNA, and green for e-lncRNA. These genes were select after global multiple testing correction (see Supplementary Tables S1, S2, S3, and S4)

Among the ubiquitously down-regulated ip-lncRNAs (see Supplementary Table S3), *LINC00478* has been previously reported in many different tumors including leukemia, breast, vulvar, prostate, and bladder cancer[16–20]. In vulvar squamous cell carcinoma, there is a statistical relationship between *LINC00478* and *MIR31HG* expression and tumor differentiation[17]. Additionally, *LINC00478* down-regulated in ER positive breast tumors was shown to be associated with progression, recurrence, and metastasis[18]. In contrast, increased expression of *SNHG17* (an ip-lncRNA, see Supplementary Table S3), was associated with short term survival in breast cancer, and with tumor size, stage, and lymph node metastasis in colorectal cancer[21,22]. Another ip-lncRNA, *AC004463*, (Supplementary Table S3), was found up-regulated in liver cancer and metastatic prostate cancer[23]. Regarding the last lncRNA category considered here, we could not find any cancer association for common e-lncRNAs, nevertheless one, *RP5-965F6*, was previously reported to be up-regulated in late-onset Alzheimer's disease[24]. The e-lncRNAs category also yielded the lowest number of genes in common among all cancer types, reinforcing the concept that lncRNAs, specially enhancers are expressed in a specific manner (Supplementary Table S4).

Finally, as a prototypical example, we considered prostate cancer (PCa), and we were able to confirm findings from previous

reports for both coding and non-coding genes (see Supplementary Figure S2). For coding genes, we confirmed differential expression for known markers of PCa progression and mortality, like *ERG*, *FOXA1*, *RNASEL*, *ARVCF*, and *SLC43A1*[25,26]. Similarly, we also confirmed differential expression for non-coding genes, like *PCA3*, the first clinically approved lncRNA marker for PCa[27,28], *PCAT1*, a prostate-specific lncRNA involved in disease progression[29], *MALAT1*, which is associated with PCa poor prognosis[30], *CDKN2B-AS1*, an anti-sense lncRNA up-regulated in PCa that inhibits tumor suppressor genes activity[31,32], and the *MIR135* host gene, which is associated with castration-resistant PCa[33].

Enhancer expression levels hold prognostic value

The number of lncRNAs involved in cancer development and progression is rapidly increasing, we therefore analyzed the prognostic value of the lncRNAs we identified in our gene expression differential analysis in TCGA, as well as those previously reported in other studies. To this end, Chen and collaborators have recently surveyed enhancers expression in nearly 9,000 patients from the TCGA[34], using genomic coordinates from the FANTOM5 project[35], identifying 4,803 enhancers with prognostic potential in one or more tumor types in the TCGA. We therefore leveraged the `FC-R2` atlas to identify prognostic coding and non-coding genes using Univariate Cox proportional hazard models, comparing our results for e-lncRNAs with those reported by Chen and colleagues.

When we considered e-lncRNAexpression levels, we identified a total of 5,382 prognostic e-lncRNAs (FDR ≤ 0.05), and no single one was predictive across all cancer types. Overall, the number of significant prognostic e-lncRNAs varied across tumors, ranging from 3 in head and neck cancer to 3,850 in kidney cancers (see Supplementary Table S6). Notably, two (out of three) e-lncRNAs from our differential gene expression consensus list across all tumor types were also prognostic. Specifically, *CATG00000107122* was associated with worst prognosis in kidney cancer, while *ENSG00000255958* was associated with worse survival in stomach tumor. Overall, despite differences in annotation and quantification (see Supplementary Table S5), we were able to confirm prognostic value for 2,765 e-lncRNAs out of the 4,803 reported by Chen et al[34], including *"enhancer 22"* (*ENSG00000272666*, which was highlighted as a promising prognostic marker for kidney cancer (Supplementary Figure S3).

Finally, we analyzed the prognostic value for dp-lncRNAs, ip-lncRNAs, and mRNAs (See Supplementary Tables S7, S8, and S9, respectively), and assessed the survival prognostic potential of our consensus genes across tumor types. Thirty-seven of the 41 coding mRNAs, 22 of the 28 differentially expressed dp-lncRNAs, and two out of the four DE ip-lncRNAs, respectively, were found to be prognostic (See Supplementary Tables S10, S11, S12, and S13). Kaplan-Meier survival curves for one selected DE gene on each RNA subtype evaluated here are shown in supplementary figure S4.

Discussion

The importance of lncRNAs in cell biology and disease has clearly emerged in the past few years and different classes of lncRNAs have been shown to play crucial roles in cell regulation and homeostasis[36]. For instance, enhancers – a major category of gene regulatory elements, which has been shown to be expressed[35,37] – play a prominent role in oncogenic processes[38,39]

and other human diseases[40,41]. Despite their importance, however, there is a scarcity of large-scale datasets investigating enhancers and other lncRNA classes, in part due to the technical difficulty in applying high-throughput techniques such as ChIP-seq and Hi-C over large cohorts, and to the use of gene models that do not account for them in transcriptomics analyses. Furthermore, the large majority of the lncRNAs that are already known – and that have been shown to be associated with some phenotype – are still lacking functional annotation.

To address these needs, the FANTOM consortium has first constructed the *FANTOM-CAT* meta-transcriptome, a comprehensive atlas of coding and non-coding genes with robust support from CAGE-seq data[4], then it has undertaken a large scale project to systematically target lncRNAs and characterize their function using a multi-pronged approach (Jordan et al., under review). In a complementary effort, we have leveraged public domain gene expression data from *recount2*[7,42] to create a comprehensive gene expression compendium across human cells and tissues based on the *FANTOM-CAT* gene model, with the ultimate goal of facilitating lncRNAs annotation through association studies.

In order to validate our resource, we have compared the gene expression summaries based on *FANTOM-CAT* gene models with previous, well-established quantification of gene expression, demonstrating virtually identical profiles across tissue types overall and for specific tissue markers. We have then confirmed that distinct classes of coding and non-coding genes differ in terms of overall expression levels and specificity patterns across cell types and tissues. Furthermore, with this approach, we were also able to identify mRNAs, promoters, enhancers, and other lncRNAs that are differentially expressed in cancer, both confirming previously reported findings, and identifying novel cancer genes exclusively annotated in the *FANTOM-CAT* gene model, which have been therefore missed in prior analyses with TCGA data. Finally, we also analyzed the prognostic value of the coding and non-coding genes we identified in our analyses, and confirmed the association with overall survival in TCGA for measurable enhancers.

Collectively, by confirming findings reported in previous studies, our results demonstrate that the `FC-R2` gene expression atlas is a reliable and powerful resource for exploring both the coding and non-coding transcriptome, providing compelling evidence and robust support to the notion that lncRNA gene classes, including enhancers and promoters, despite not being yet fully understood, portend significant biological functions. Our resource, therefore, constitutes a suitable and promising platform for future large scales studies in cancer and other human diseases, which in turn hold the potential to reveal important cues to the understanding of their biological, physiological, and pathological roles, potentially leading to improved diagnostic and therapeutic interventions.

Finally, all results and data from the `FC-R2` atlas are available as a public tool. With uniformly processed expression data for over 70,000 samples and 109,873 genes ready to analyze, we want to encourage researchers to dive deeper into the study of ncRNAs, their interaction with coding and non-coding genes, and their influence on normal and disease tissues. We hope this new resource will help paving the way to develop new hypotheses that can be followed to unwind the biological role of the transcriptome as a whole.

Methods

Data and pre-processing.

FANTOM CAT permissive catalog was obtained from the pre-FANTOM6 consortium. This catalog initially comprised 124,245 genes defined by CAGE peaks published by Hon et al[4]. In order to remove ambiguity, BED files containing the coordinates for each gene/exon were imported into an R session and processed with the GenomicRanges package[43] by disjoining the exon coordinates. To avoid losing strand information we processed it in a two-step approach by first disjoining overlapping segments on the same strand and latter across strands (Figure 5). Genomic ranges (disjoined exons segments) that mapped back to more than one gene were discarded. The expression values for these ranges were then quantified using *recount.bwtool*[44] (code at `https://github.com/LieberInstitute/marchionni_projects`). The resulting expression quantifications were processed to generate `RangedSummarizedExperiment` objects compatible with the *recount2* framework[7,42] (code at `https://github.com/eddieimada/fcr2`). Thus `FC-R2` provides expression information for coding mRNAs, enhancers and promoters (divergent and intergenic) for 9,662 samples from the Genotype-Tissue Expression (GTEx) project, 11,350 samples from The Cancer Genome Atlas (TCGA) consortium, and over 50,000 samples from the Sequence Read Archive (SRA).

Correlation with other studies.

To test if the pre-processing step had a major impact on expression quantification, we compared our counts tables to the published GTEx counts from *recount2*. The version 2 of the gene counts for the GTEx samples were downloaded from the recount website (`https://jhubiostatistics.shinyapps.io/recount/`). We compared distribution of tissue specific genes across tissues and computed the Pearson correlation for each gene in common across the original *recount2* gene counts estimates and our version.

Expression specificity of tissue facets.

We analyzed the expression level and specificity of each gene stratified by RNA class (i.e. mRNA, e-lncRNA, dp-lncRNA, ip-lncRNA). Expression levels for each gene were represented by the maximum transcripts per million (TPM) of all samples within a facet. To compute the gene specificity we followed the same approach used in Hon et al[4]. The 99.99 percent confidence intervals for the expression of each category by facet were calculated based on TPM values. Genes with a TPM greater than 0.01 were considered expressed.

Identification of differentially expressed genes.

Differential gene expression was tested in 13 cancer types, comparing primary tumor with normal samples using TCGA `FC-R2` gene expression summaries. Summaries for each cancer type were split by RNA class (coding mRNA, intergenic promoter lncRNA, divergent promoter lncRNA and enhancer lncRNA) and analyzed independently. A generalized linear model approach coupled with empirical Bayes standard errors[45] was used to identify differentially expressed genes between the samples. The

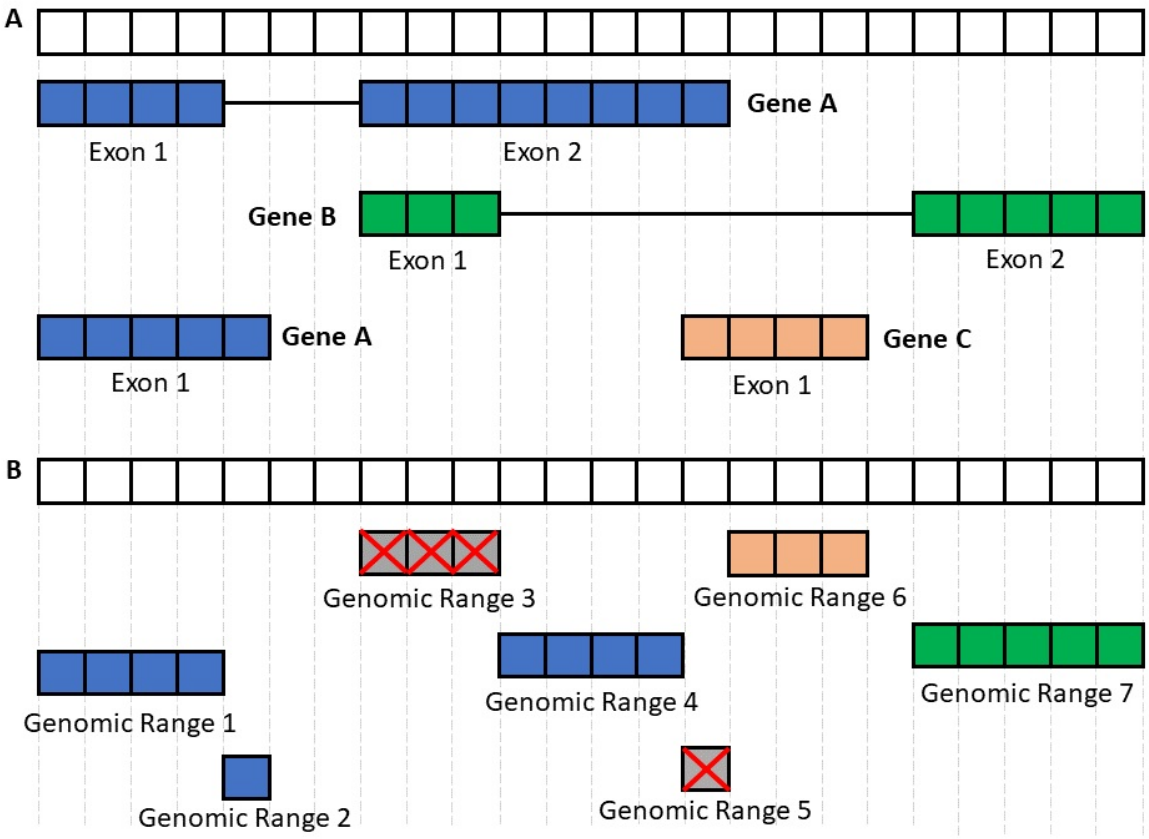

Figure 5. FANTOM-CAT genomic ranges. Representation of the disjoining and exon disambiguation processes. (A) Representation of a genome segment and its annotation containing 3 genes with gene A having two isoforms, and genes B and C with one isoform each. Each box can be interpreted as one nucleotide with boxes colored blue or orange to represent exons on opposite strands. (B) Representation of disjoined exon ranges from example A. Each feature is reduced to a set of non-overlapping genomic ranges, then genomic ranges mapping back to two or more genes are removed (crossed boxes). After removal of ambiguous ranges, the remaining ranges are summarized at gene level. Grey boxes represent segments with ambiguous strand.

model was adjusted for the three most variable coefficients for data heterogeneity as estimated by surrogate variable analysis (SVA)[46]. Correction for multiple testing was performed across RNA classes by merging the resulting p-values for each cancer type and applying the Benjamini-Hochberg method[47].

Prognostic analysis.

To evaluate the prognostic potential of the genes in `FC-R2`we applied a univariate Cox proportional regression model in four RNA classes (22106 mRNAs, 17,404 e-lncRNAs, 6,204 dp-lncRNAs, and 1,948 ip-lncRNAs) comprised in `FC-R2` across each of the 13 TCGA cancer types with available survival follow-up. Genes with FDR equal or less than 0.05 using Benjamini-Hochberg[47] correction within the cancer type and RNA class, were selected as significant prognostic factors. To indentify differentially expressed genes that portrait predictive potential, the DE lists were intersected with the significant prognostic genes lists. Supplementary data from Chen et al[34] containing enhancers position and prognostic potential were

obtained from the original publication and a liftover to hg38 genome assembly was performed to match FC−R2 coordinates in order to compare the results.

Data Availability

All data is available in http://marchionnilab.org/fcr2.html. Expression data can be directly accessed through https://jhubiostatistics.shinyapps.io/recount/ and the *recount* Bioconductor package (v1.9.5 or newer) at https://bioconductor.org/packages/recount as *RangedSummarizedExperiment* objects organized by The Sequence Read Archive (SRA) study ID. The data can be loaded using R-programming language and is ready to be analyzed using Bioconductor packages or the data can be exported to other formats for use in another environment.

Code Availability

All code used in this manuscript is available in: https://github.com/eddieimada/fcr2 and https://github.com/LieberInstitute/marchionni_projects for reproducibility purposes.

Acknowledgements

This publication was made possible though support from the NIH-NCI grants P30CA006973 (L.M. and A.F.) and R01CA200859 (W.D. and L.M.), NIH-NIGMS grant R01GM118568 (C.W. and B.L.), R21MH109956-01 (L.C.T. and A.E.J.), and the Department of Defense (DoD) office of the Congressionally Directed Medical Research Programs (CDMRP) award W81XWH-16-1-0739 (E.L.I. and L.M.), RFBR 17-00-00208 (A.F.) and Russian Academic project 0112-2019-0001 (A.F.), Fundação de Amparo à Pesquisa do Estado de Minas Gerais award BDS-00493-16 (E.L.I and G.R.F.). *recount2* and FC−R2 are hosted on SciServer, a collaborative research environment for large-scale data-driven science. It is being developed at, and administered by, the Institute for Data Intensive Engineering and Science (IDIES) at Johns Hopkins University. SciServer is funded by the National Science Foundation Award ACI-1261715. For more information about SciServer, visit http://www.sciserver.org/.

Author contributions statement

L.M. conceived the idea, L.M., E.I., A.F. and B.L. designed the study; E.L.I., D.F.S., T.M., W.D., A.S., L.C.T., and L.M. performed the analysis; E.L.I., D.F.S., F.P.L., G.R.F. and L.M. interpreted the results; L.C.T., C.W., C.Y., K.Y, N.K., M.I., H.S., T.K., C.C.H., M.H., J.W.S., P.C. A.E.J., J.T.L. and B.L. provided the data and tools; E.L.I., D.F.S., L.C.T., B.L. and L.M. wrote the manuscript; All authors reviewed and approved the manuscript.

Disclosure declaration

All authors declare no conflicts of interest.

References

1. Batista, P. J. & Chang, H. Y. Long noncoding RNAs: cellular address codes in development and disease. Cell **152**, 1298–1307 (2013). URL http://eutils.ncbi.nlm.nih.gov/entrez/eutils/elink.fcgi?dbfrom=pubmed&id=23498938&retmode=ref&cmd=prlinks. DOI 10.1016/j.cell.2013.02.012.

2. Esteller, M. Non-coding RNAs in human disease. Nat. reviews Genet. **12**, 861–874 (2011). URL https://www.nature.com/articles/nrg3074. DOI 10.1038/nrg3074.

3. Ling, H. et al. Junk DNA and the long non-coding RNA twist in cancer genetics. Oncogene **34**, 5003–5011 (2015). URL http://www.nature.com/articles/onc2014456. DOI 10.1038/onc.2014.456.

4. Hon, C.-C. et al. An atlas of human long non-coding RNAs with accurate 5' ends. Nat. **543**, 199–204 (2017). URL http://www.nature.com/doifinder/10.1038/nature21374. DOI 10.1038/nature21374.

5. Lachmann, A. et al. Massive mining of publicly available RNA-seq data from human and mouse. Nat Commun **9**, 1366 (2018).

6. Tatlow, P. J. & Piccolo, S. R. A cloud-based workflow to quantify transcript-expression levels in public cancer compendia. Sci Rep **6**, 39259 (2016).

7. Collado-Torres, L. et al. Reproducible RNA-seq analysis using recount2. Nat. Biotechnol. **35**, 319–321 (2017). URL http://www.nature.com/doifinder/10.1038/nbt.3838. DOI 10.1038/nbt.3838.

8. Network, C. G. A. R. et al. The Cancer Genome Atlas Pan-Cancer analysis project. Nat. Genet. **45**, 1113–1120 (2013). URL http://eutils.ncbi.nlm.nih.gov/entrez/eutils/elink.fcgi?dbfrom=pubmed&id=24071849&retmode=ref&cmd=prlinks. DOI 10.1038/ng.2764.

9. GTEx Consortium. The Genotype-Tissue Expression (GTEx) project. Nat. Genet. **45**, 580–585 (2013). URL http://www.nature.com/articles/ng.2653. DOI 10.1038/ng.2653.

10. Ong, C.-T. & Corces, V. G. Enhancer function: new insights into the regulation of tissue-specific gene expression. Nat. Rev. Genet. **12**, 283 (2011).

11. Zhou, M. et al. Lncrna-hh strengthen cancer stem cells generation in twist-positive breast cancer via activation of hedgehog signaling pathway. Stem cells **34**, 55–66 (2016).

12. Zhao, J. et al. Long non-coding rna linc00152 is involved in cell cycle arrest, apoptosis, epithelial to mesenchymal transition, cell migration and invasion in gastric cancer. Cell cycle **14**, 3112–3123 (2015).

13. Shang, D., Zheng, T., Zhang, J., Tian, Y. & Liu, Y. Profiling of mrna and long non-coding rna of urothelial cancer in recipients after renal transplantation. Tumor Biol. **37**, 12673–12684 (2016).

14. Cao, W.-J., Wu, H.-L., He, B.-S., Zhang, Y.-S. & Zhang, Z.-Y. Analysis of long non-coding rna expression profiles in gastric cancer. World journal gastroenterology: WJG **19**, 3658 (2013).

15. Sun, Y. et al. The long noncoding rna snhg1 promotes tumor growth through regulating transcription of both local and distal genes. Oncogene **36**, 6774 EP – (2017). URL https://doi.org/10.1038/onc.2017.286.

16. Emmrich, S. et al. Lincrnas monc and mir100hg act as oncogenes in acute megakaryoblastic leukemia. Mol. cancer **13**, 1 (2014).

17. Ni, S., Zhao, X. & Ouyang, L. Long non-coding rna expression profile in vulvar squamous cell carcinoma and its clinical significance. Oncol. reports **36**, 2571–2578 (2016).

18. Gökmen-Polar, Y. et al. Abstract p2-06-05: Linc00478: A novel tumor suppressor in breast cancer (2016).

19. Sun, D. et al. Regulation of several androgen-induced genes through the repression of the mir-99a/let-7c/mir-125b-2 mirna cluster in prostate cancer cells. Oncogene **33**, 1448 (2014).

20. Li, S. et al. Exploring functions of long noncoding rnas across multiple cancers through co-expression network. Sci. reports **7**, 754 (2017).

21. Zhao, W., Luo, J. & Jiao, S. Comprehensive characterization of cancer subtype associated long non-coding rnas and their clinical implications. Sci. reports **4**, 6591 (2014).

22. Ma, Z. et al. Long non-coding rna snhg17 is an unfavourable prognostic factor and promotes cell proliferation by epigenetically silencing p57 in colorectal cancer. Mol. BioSystems **13**, 2350–2361 (2017).

23. Zhu, S. et al. Genome-scale deletion screening of human long non-coding rnas using a paired-guide rna crispr–cas9 library. Nat. biotechnology **34**, 1279 (2016).

24. Humphries, C. E. et al. Integrated whole transcriptome and dna methylation analysis identifies gene networks specific to late-onset alzheimer's disease. J. Alzheimer's Dis. **44**, 977–987 (2015).

25. Lin, D. W. et al. Genetic variants in the LEPR, CRY1, RNASEL, IL4, and ARVCF genes are prognostic markers of prostate cancer-specific mortality. Cancer Epidemiol Biomarkers Prev **20**, 1928–1936 (2011). URL http://cebp.aacrjournals.org/content/20/9/1928.abstract. DOI 10.1158/1055-9965.EPI-11-0236.

26. Yu, J. et al. An integrated network of androgen receptor, polycomb, and TMPRSS2-ERG gene fusions in prostate cancer progression. Cancer cell **17**, 443–454 (2010). URL http://www.sciencedirect.com/science?_ob=ArticleURL&_udi=B6WWK-503HV0F-7&_user=75682&_coverDate=05%2F18%2F2010&_rdoc=1&_fmt=high&_orig=gateway&_origin=gateway&_sort=d&_docanchor=&view=c&_acct=C000006078&_version=1&_urlVersion=0&_userid=75682&md5=1893cfe1116f128f58fa146786f4e208&searchtype=a. DOI 10.1016/j.ccr.2010.03.018.

27. Bussemakers, M. J. et al. DD3: a new prostate-specific gene, highly overexpressed in prostate cancer. Cancer Res. **59**, 5975–5979 (1999).

28. de Kok, J. B. et al. DD3(PCA3), a very sensitive and specific marker to detect prostate tumors. Cancer Res **62**, 2695–2698 (2002). URL http://eutils.ncbi.nlm.nih.gov/entrez/eutils/elink.fcgi?dbfrom=pubmed&id=11980670&retmode=ref&cmd=prlinks.

29. Prensner, J. R. et al. Transcriptome sequencing across a prostate cancer cohort identifies PCAT-1, an unannotated lincRNA implicated in disease progression. Nat. Biotechnol. **29**, 742–749 (2011). URL http://www.nature.com/articles/nbt.1914. DOI 10.1038/nbt.1914.

30. Ren, S. et al. Long noncoding RNA MALAT-1 is a new potential therapeutic target for castration resistant prostate cancer. The J. Urol. **190**, 2278–2287 (2013). URL http://eutils.ncbi.nlm.nih.gov/entrez/eutils/elink.fcgi?dbfrom=pubmed&id=23845456&retmode=ref&cmd=prlinks. DOI 10.1016/j.juro.2013.07.001.

31. Gutschner, T. & Diederichs, S. The hallmarks of cancer: a long non-coding RNA point of view. RNA Biol **9**, 703–719 (2012). URL http://eutils.ncbi.nlm.nih.gov/entrez/eutils/elink.fcgi?dbfrom=pubmed&id=22664915&retmode=ref&cmd=prlinks. DOI 10.4161/rna.20481.

32. Kotake, Y. et al. Long non-coding RNA ANRIL is required for the PRC2 recruitment to and silencing of p15(INK4B) tumor suppressor gene. Oncogene **30**, 1956–1962 (2011). URL https://www.nature.com/articles/onc2010568. DOI 10.1038/onc.2010.568.

33. Huang, X. et al. Exosomal miR-1290 and miR-375 as prognostic markers in castration-resistant prostate cancer. Eur. urology **67**, 33–41 (2015). URL http://linkinghub.elsevier.com/retrieve/pii/S0302283814006873. DOI 10.1016/j.eururo.2014.07.035.

34. Chen, H., Li, C., Peng, X., Zhou, Z., Weinstein, J. N., Liang, H. A promoter-level mammalian expression atlas. Cell **173**, 386–399 (2018).

35. Andersson, R. et al. An atlas of active enhancers across human cell types and tissues. Nat. **507**, 455–461 (2014). URL http://eutils.ncbi.nlm.nih.gov/entrez/eutils/elink.fcgi?dbfrom=pubmed&id=24670763&retmode=ref&cmd=prlinks. DOI 10.1038/nature12787.

36. Quinn, J. J. & Chang, H. Y. Unique features of long non-coding rna biogenesis and function. Nat. Rev. Genet. **17**, 47 (2016).

37. Arner, E. et al. Transcribed enhancers lead waves of coordinated transcription in transitioning mammalian cells. Sci. (New York, NY) (2015). URL http://eutils.ncbi.nlm.nih.gov/entrez/eutils/elink.fcgi?dbfrom=pubmed&id=25678556&retmode=ref&cmd=prlinks. DOI 10.1126/science.1259418.

38. Sur, I. & Taipale, J. The role of enhancers in cancer. Nat. Rev. Cancer **16**, 483 (2016).

39. Herz, H.-M., Hu, D. & Shilatifard, A. Enhancer malfunction in cancer. Mol. cell **53**, 859–866 (2014).

40. Blencowe, B. J. Exonic splicing enhancers: mechanism of action, diversity and role in human genetic diseases. Trends biochemical sciences **25**, 106–110 (2000).

41. Hnisz, D. et al. Super-enhancers in the control of cell identity and disease. Cell **155**, 934–947 (2013).

42. Collado-Torres, L., Nellore, A. & Jaffe, A. E. recount workflow: Accessing over 70,000 human RNA-seq samples with Bioconductor. F1000Research **6**, 1558 (2017). URL https://f1000research.com/articles/6-1558/v1. DOI 10.12688/f1000research.12223.1.

43. Lawrence, M. et al. Software for computing and annotating genomic ranges. PLoS Comput. Biol. **9**, e1003118 (2013). URL http://eutils.ncbi.nlm.nih.gov/entrez/eutils/elink.fcgi?dbfrom=pubmed&id=23950696&retmode=ref&cmd=prlinks. DOI 10.1371/journal.pcbi.1003118.

44. Ellis, S. E., Collado-Torres, L., Jaffe, A. & Leek, J. T. Improving the value of public RNA-seq expression data by phenotype prediction. Nucleic Acids Res. **46**, e54–e54 (2018). URL https://doi.org/10.1093/nar/gky102. DOI 10.1093/nar/gky102. http://oup.prod.sis.lan/nar/article-pdf/46/9/e54/24829382/gky102.pdf.

45. Smyth, G. K. Linear models and empirical bayes methods for assessing differential expression in microarray experiments. Stat. applications genetics molecular biology **3**, Article3 (2004). URL http://www.ncbi.nlm.nih.gov/pubmed/16646809?dopt=abstract. DOI 10.2202/1544-6115.1027.

46. Leek, J. T. & Storey, J. D. Capturing heterogeneity in gene expression studies by surrogate variable analysis. PLoS genetics **3**, 1724–1735 (2007). URL http://www.plosgenetics.org/article/info%3Adoi%2F10.1371%2Fjournal.pgen.0030161. DOI 10.1371/journal.pgen.0030161.

47. Benjamini, Y. & Hochberg, Y. Controlling the false discovery rate: a practical and powerful approach to multiple testing. J. Royal Stat. Soc. **Series B, 57**, 289–300 (1995). URL http://www.dm.uba.ar/materias/analisis_expl_y_conf_de_datos_de_exp_de_marrays_Mae/2006/1/teoricas/FDR%201995.pdf.

48. Buja, A. & Eyuboglu, N. Remarks on parallel analysis. Multivar. behavioral research **27**, 509–540 (1992).

49. Therneau, T. M. A Package for Survival Analysis in S (2015). URL https://CRAN.R-project.org/package=survival. Version 2.38.

50. Kassambara, A. & Kosinski, M. survminer: Drawing Survival Curves using 'ggplot2' (2018). URL https://CRAN.R-project.org/package=survminer. R package version 0.4.3.

Supplementary Information

Recounting the FANTOM Cage Associated Transcriptome

Eddie-Luidy Imada, Diego Fernando Sanchez, Leonardo Collado-Torres, Christopher Wilks, Tejasvi Matam, Wikum Dinalankara, Aleksey Stupnikov, Francisco Lobo-Pereira, Chi-Wai Yip, Kayoko Yasuzawa, Naoto Kondo, Masayoshi Itoh, Harukazu Suzuki, Takeya Kasukawa, Chung Chau Hon, Michiel de Hoon, Jay W Shin, Piero Carninci, FANTOM consortium, Andrew E Jaffe, Jeffrey T Leek, Alexander Favorov, Gloria R Franco, Ben Langmead, and Luigi Marchionni

Supplementary Tables

Table S1. Intersection of significant mRNA across 13 cancer types (Global FDR < 0.000001)

geneID	geneSymbol	geneType	CAT_geneClass	CAT_DHS_type	Chromosome	geneStart	geneEnd	strand	Direction
ENSG00000065328	MCM10	protein_coding	coding_mRNA	DHS_promoter	chr10	13161579	13211916	+	Up-regulated in tumor
ENSG00000090889	KIF4A	protein_coding	coding_mRNA	DHS_promoter	chrX	70290040	70421061	+	Up-regulated in tumor
ENSG00000091651	ORC6	protein_coding	coding_mRNA	DHS_promoter	chr16	46689310	46702149	+	Up-regulated in tumor
ENSG00000092853	CLSPN	protein_coding	coding_mRNA	DHS_promoter	chr1	35719788	35769967	-	Up-regulated in tumor
ENSG00000093009	CDC45	protein_coding	coding_mRNA	DHS_promoter	chr22	19479466	19528387	+	Up-regulated in tumor
ENSG00000100162	CENPM	protein_coding	coding_mRNA	DHS_promoter	chr22	41769677	41947123	-	Up-regulated in tumor
ENSG00000102384	CENPI	protein_coding	coding_mRNA	DHS_promoter	chrX	101098204	101169831	+	Up-regulated in tumor
ENSG00000105011	ASF1B	protein_coding	coding_mRNA	DHS_promoter	chr19	14118278	14138467	-	Up-regulated in tumor
ENSG00000106268	NUDT1	protein_coding	coding_mRNA	DHS_promoter	chr7	2242226	2251354	+	Up-regulated in tumor
ENSG00000112984	KIF20A	protein_coding	coding_mRNA	DHS_promoter	chr5	138178724	138189480	+	Up-regulated in tumor
ENSG00000115163	CENPA	protein_coding	coding_mRNA	DHS_promoter	chr2	26764321	26803376	+	Up-regulated in tumor
ENSG00000117650	NEK2	protein_coding	coding_mRNA	DHS_promoter	chr1	211658373	211675621	-	Up-regulated in tumor
ENSG00000121152	NCAPH	protein_coding	coding_mRNA	DHS_promoter	chr2	96335801	96393940	+	Up-regulated in tumor
ENSG00000126787	DLGAP5	protein_coding	coding_mRNA	DHS_promoter	chr14	55148112	55191585	-	Up-regulated in tumor
ENSG00000138180	CEP55	protein_coding	coding_mRNA	DHS_promoter	chr10	93496639	93546919	+	Up-regulated in tumor
ENSG00000144554	FANCD2	protein_coding	coding_mRNA	DHS_promoter	chr3	10023970	10102460	+	Up-regulated in tumor
ENSG00000148773	MKI67	protein_coding	coding_mRNA	DHS_promoter	chr10	128092566	128126423	-	Up-regulated in tumor
ENSG00000156970	BUB1B	protein_coding	coding_mRNA	DHS_promoter	chr15	40161069	40223524	+	Up-regulated in tumor
ENSG00000157456	CCNB2	protein_coding	coding_mRNA	DHS_promoter	chr15	59097077	59161020	+	Up-regulated in tumor
ENSG00000162062	C16orf59	protein_coding	coding_mRNA	DHS_dyadic	chr16	2460109	2465114	+	Up-regulated in tumor
ENSG00000165304	MELK	protein_coding	coding_mRNA	DHS_promoter	chr9	36572085	36682572	+	Up-regulated in tumor
ENSG00000166508	MCM7	protein_coding	coding_mRNA	DHS_promoter	chr7	100085474	100105533	-	Up-regulated in tumor
ENSG00000167513	CDT1	protein_coding	coding_mRNA	DHS_promoter	chr16	88799649	88818226	+	Up-regulated in tumor
ENSG00000169679	BUB1	protein_coding	coding_mRNA	DHS_promoter	chr2	110630642	110678063	-	Up-regulated in tumor
ENSG00000186185	KIF18B	protein_coding	coding_mRNA	DHS_promoter	chr17	44923253	44947773	-	Up-regulated in tumor
ENSG00000189057	FAM111B	protein_coding	coding_mRNA	DHS_promoter	chr11	59063500	59131211	+	Up-regulated in tumor
ENSG00000076555	ACACB	protein_coding	coding_mRNA	DHS_enhancer	chr12	109116443	109270766	+	Down-regulated in tumor
ENSG00000106034	CPED1	protein_coding	coding_mRNA	DHS_promoter	chr7	120987841	121310413	+	Down-regulated in tumor
ENSG00000112425	EPM2A	protein_coding	coding_mRNA	DHS_promoter	chr6	145382951	145763619	-	Down-regulated in tumor
ENSG00000116678	LEPR	protein_coding	coding_mRNA	DHS_promoter	chr1	65420701	65643153	+	Down-regulated in tumor
ENSG00000130988	RGN	protein_coding	coding_mRNA	DHS_promoter	chrX	47078366	47104867	+	Down-regulated in tumor
ENSG00000133800	LYVE1	protein_coding	coding_mRNA	DHS_enhancer	chr11	10307853	10611707	-	Down-regulated in tumor
ENSG00000136842	TMOD1	protein_coding	coding_mRNA	DHS_promoter	chr9	97501142	97628196	+	Down-regulated in tumor
ENSG00000138356	AOX1	protein_coding	coding_mRNA	DHS_promoter	chr2	200586053	200677064	+	Down-regulated in tumor

Continued on next page

Table S1. Intersection of significant mRNA across 13 cancer types (Global FDR < 0.000001)

geneID	geneSymbol	geneType	CAT_geneClass	CAT_DHS_type	Chromosome	geneStart	geneEnd	strand	Direction
ENSG00000151623	NR3C2	protein_coding	coding_mRNA	DHS_promoter	chr4	148077496	148445575	-	Down-regulated in tumor
ENSG00000154330	PGM5	protein_coding	coding_mRNA	DHS_promoter	chr9	68327407	68539746	+	Down-regulated in tumor
ENSG00000168546	GFRA2	protein_coding	coding_mRNA	DHS_promoter	chr8	21365101	21812338	-	Down-regulated in tumor
ENSG00000170271	FAXDC2	protein_coding	coding_mRNA	DHS_promoter	chr5	154810519	154859509	-	Down-regulated in tumor
ENSG00000185432	METTL7A	protein_coding	coding_mRNA	DHS_promoter	chr12	50922629	50935894	+	Down-regulated in tumor
ENSG00000196616	ADH1B	protein_coding	coding_mRNA	DHS_enhancer	chr4	99286865	99321401	-	Down-regulated in tumor
ENSG00000198300	PEG3	protein_coding	coding_mRNA	DHS_promoter	chr19	56801328	56840726	-	Down-regulated in tumor

Table S2. Intersection of significant divergent promoters across 13 cancer types (Global FDR < 0.1)

geneID	geneSymbol	geneType	CAT_geneClass	CAT_DHS_type	Chromosome	geneStart	geneEnd	strand	Direction
CATG00000017193	CATG00000017193.1	__na	lncRNA_divergent	DHS_promoter	chr13	52649609	52652307	-	Up-regulated in tumor
CATG00000020461	CATG00000020461.1	__na	lncRNA_divergent	DHS_promoter	chr14	22831988	22836822	-	Up-regulated in tumor
CATG00000054098	CATG00000054098.1	__na	lncRNA_divergent	DHS_promoter	chr20	3043468	3048131	-	Up-regulated in tumor
CATG00000087995	CATG00000087995.1	__na	lncRNA_divergent	DHS_promoter	chr6	30639697	30647759	-	Up-regulated in tumor
CATG00000101363	CATG00000101363.1	__na	lncRNA_divergent	DHS_promoter	chr8	144792564	144796174	+	Up-regulated in tumor
ENSG00000228839	RP3-400N23.6	antisense	lncRNA_divergent	DHS_promoter	chr22	31290906	31357952	+	Up-regulated in tumor
ENSG00000235989	MORC2-AS1	antisense	lncRNA_divergent	DHS_promoter	chr22	30922325	30932449	+	Up-regulated in tumor
ENSG00000247373	RP11-486O12.2	lincRNA	lncRNA_divergent	DHS_promoter	chr12	123575002	123584820	-	Up-regulated in tumor
ENSG00000255717	SNHG1	processed_transcript	lncRNA_divergent	DHS_promoter	chr11	62851874	62855885	-	Up-regulated in tumor
ENSG00000257605	RP11-680A11.5	antisense	lncRNA_divergent	DHS_promoter	chr12	53298394	53300360	-	Up-regulated in tumor
ENSG00000258384	AC068831.6	antisense	lncRNA_divergent	DHS_promoter	chr15	90950782	90955229	-	Up-regulated in tumor
ENSG00000260442	RP11-22P6.3	antisense	lncRNA_divergent	DHS_promoter	chr16	28868384	28879920	-	Up-regulated in tumor
ENSG00000263412	RP5-890E16.2	processed_transcript	lncRNA_divergent	DHS_promoter	chr17	48038796	48048670	-	Up-regulated in tumor
ENSG00000270195	RP11-572O17.1	lincRNA	lncRNA_divergent	DHS_promoter	chr4	1712410	1715967	+	Up-regulated in tumor
ENSG00000272455	RP4-758J18.13	lincRNA	lncRNA_divergent	DHS_promoter	chr1	1407377	1410854	+	Up-regulated in tumor
CATG00000105517	CATG00000105517.1	__na	lncRNA_divergent	DHS_promoter	chr9	70413086	70609298	+	Down-regulated in tumor
ENSG00000175611	LINC00476	processed_transcript	lncRNA_divergent	DHS_promoter	chr9	95759231	95875979	-	Down-regulated in tumor
ENSG00000225793	RP1-234P15.4	lincRNA	lncRNA_divergent	DHS_promoter	chr6	75284598	75305766	+	Down-regulated in tumor
ENSG00000226237	RP11-276H19.1	lincRNA	lncRNA_divergent	DHS_promoter	chr9	86946617	87014413	+	Down-regulated in tumor
ENSG00000232160	RAP2C-AS1	antisense	lncRNA_divergent	DHS_promoter	chrX	132217007	132435459	+	Down-regulated in tumor
ENSG00000234492	RPL34-AS1	lincRNA	lncRNA_divergent	DHS_promoter	chr4	108538190	108620395	-	Down-regulated in tumor
ENSG00000235652	RP11-545I5.3	antisense	lncRNA_divergent	DHS_promoter	chr6	145814895	145886585	+	Down-regulated in tumor

Continued on next page

Table S2. Intersection of significant divergent promoters across 13 cancer types (Global FDR < 0.1)

geneID	geneSymbol	geneType	CAT_geneClass	CAT_DHS_type	Chromosome	geneStart	geneEnd	strand	Direction
ENSG00000245293	RP11-286E11.1	antisense	lncRNA_divergent	DHS_promoter	chr4	107862676	107989692	-	Down-regulated in tumor
ENSG00000248866	USP46-AS1	lincRNA	lncRNA_divergent	DHS_promoter	chr4	52656631	52669444	+	Down-regulated in tumor
ENSG00000248980	RP11-87F15.2	antisense	lncRNA_divergent	DHS_promoter	chr4	176303507	176322213	-	Down-regulated in tumor
ENSG00000267414	RP11-456K23.1	lincRNA	lncRNA_divergent	DHS_promoter	chr18	44664515	44680693	-	Down-regulated in tumor
ENSG00000271849	CTC-332L22.1	lincRNA	lncRNA_divergent	DHS_promoter	chr5	109687802	109689251	-	Down-regulated in tumor
ENSG00000272686	RP11-390E23.6	antisense	lncRNA_divergent	DHS_promoter	chr7	123748542	123756392	+	Down-regulated in tumor

Table S3. Intersection of significant intergenic promoters across 13 cancer types (Global FDR < 0.1)

geneID	geneSymbol	geneType	CAT_geneClass	CAT_DHS_type	Chromosome	geneStart	geneEnd	strand	Direction
ENSG00000196756	SNHG17	processed_transcript	lncRNA_intergenic	DHS_promoter	chr20	38404766	38435328	-	Up-regulated in tumor
ENSG00000260924	AC004463.6	antisense	lncRNA_intergenic	DHS_promoter	chr22	19171395	19175403	+	Up-regulated in tumor
ENSG00000215386	LINC00478	lincRNA	lncRNA_intergenic	DHS_promoter	chr21	15910380	16646424	+	Down-regulated in tumor
ENSG00000263753	LINC00667	lincRNA	lncRNA_intergenic	DHS_promoter	chr18	5237844	5251731	+	Down-regulated in tumor

Table S4. Intersection of significant enhancers across 13 cancer types (Global FDR < 0.1)

geneID	geneSymbol	geneType	CAT_geneClass	CAT_DHS_type	Chromosome	geneStart	geneEnd	strand	Direction
CATG00000107122	CATG00000107122.1	__na	lncRNA_antisense	DHS_enhancer	chr9	128118082	128124306	+	Up-regulated in tumor
ENSG00000231246	RP5-965F6.2	lincRNA	lncRNA_intergenic	DHS_enhancer	chr1	112176973	112360607	-	Down-regulated in tumor
ENSG00000255958	RP11-656E20.5	antisense	lncRNA_antisense	DHS_enhancer	chr12	10214161	10220555	-	Down-regulated in tumor

	Exonic	Intronic
d-lncRNA	1762	1665
i-lncRNA	1066	274
mRNA	10509	7254
other-RNA	7512	2121
pseudogene	1218	208
senseOverlap-RNA	2631	150
small-RNA	845	68
Total	34282	12247

Table S5. Remaping of Anderson's enhancers list to the FANTOM-CAT permissive set. Since originally published, many of enhancers contained in the Anderson's list[35], were reassigned or removed during the assembly of the FANTOM-CAT based on further evidence from the additional transcriptomic datasets used in the meta-assembly, as well as due to the information obtained from orthogonal genomic and epigenomic information, such as DNase I hypersensitivity and other epigenomic marks, as obtained from the Roadmap Epigenomics Project. Based on the new gene models in *FANTOM-CAT*, we verified the overlapping between the original enhancers list and then summarized the results according to current RNA classes in the *FANTOM-CAT*. The counts for the original enhancers that overlap with exons in the FANTOM-CAT gene models are shown in the "Exonic" column on the left. The counts for the enhancers that did not map to any exon, but that were still within the gene boundaries are shown in the "Intronic" column on the right.

Table S6. Survival analysis using Cox proportional regression showing the number of e-lncRNAs with prognostic value accross the 13 cancer types. *Non-significant* column indicates the number of genes with FDR greater than 0.05. *Cases* represents the number patients at the beginning of follow-up for each tumor type. *Events* is the number of death cases during follow up. *Median time* is given in days.

Tumor type	Non-significant	FDR < 0.05	Cases	Events	Median time
Kidney	13554	3850	881	227	N.A.
Uterus	16563	831	596	125	3365
Stomach	16850	554	392	158	940
Liver	16970	369	365	130	1694
Bladder	17234	153	407	178	1008
Thyroid	17277	111	504	16	N.A.
Breast	17305	96	1080	151	3941
Colorectal	17292	87	602	128	2532
Lung	17335	69	998	395	1531
Prostate	17332	53	496	10	N.A.
HeadNeck	17398	3	501	217	1671
Bile	15725	0	36	18	1220
Esophagus	17404	0	184	77	784

Table S7. Survival analysis using Cox proportional regression showing the number of dp-lncRNAs with prognostic value accross the 13 cancer types. *Non-significant* column indicates the number of genes with FDR greater than 0.05. *Cases* represents the number patients at the beginning of follow-up for each tumor type. *Events* is the number of death cases during follow up. *Median time* is given in days.

Tumor type	Non-significant	FDR < 0.05	Cases	Events	Median time
Kidney	4247	1957	881	227	N.A.
Uterus	5477	726	596	125	3365
Liver	5971	223	365	130	1694
Thyroid	6073	128	504	16	N.A.

Continued on next page

Table S7. Survival analysis using Cox proportional regression showing the number of dp-lncRNAs with prognostic value accross the 13 cancer types. *Non-significant* column indicates the number of genes with FDR greater than 0.05. *Cases* represents the number patients at the beginning of follow-up for each tumor type. *Events* is the number of death cases during follow up. *Median time* is given in days.

Tumor type	Non-significant	FDR < 0.05	Cases	Events	Median time
Prostate	6134	69	496	10	N.A.
Colorectal	6161	41	602	128	2532
Stomach	6167	37	392	158	940
Bladder	6176	27	407	178	1008
Breast	6195	8	1080	151	3941
Lung	6202	2	998	395	1531
Bile	6078	0	36	18	1220
Esophagus	6204	0	184	77	784
HeadNeck	6204	0	501	217	1671

Table S8. Survival analysis using Cox proportional regression showing the number of ip-lncRNAs with prognostic value accross the 13 cancer types. *Non-significant* column indicates the number of genes with FDR greater than 0.05. *Cases* represents the number patients at the beginning of follow-up for each tumor type. *Events* is the number of death cases during follow up. *Median time* is given in days.

Tumor type	Non-significant	FDR < 0.05	Cases	Events	Median time
Kidney	1471	477	881	227	N.A.
Uterus	1660	287	596	125	3365
Liver	1864	78	365	130	1694
Colorectal	1896	46	602	128	2532
Thyroid	1909	37	504	16	N.A.
Stomach	1919	29	392	158	940
Bladder	1930	18	407	178	1008
Prostate	1929	18	496	10	N.A.
Breast	1931	17	1080	151	3941
Lung	1938	9	998	395	1531
HeadNeck	1944	3	501	217	1671
Bile	1866	0	36	18	1220
Esophagus	1947	0	184	77	784

Table S9. Survival analysis using Cox proportional regression showing the number of mRNAs with prognostic value accross the 13 cancer types. *Non-significant* column indicates the number of genes with FDR greater than 0.05. *Cases* represents the number patients at the beginning of follow-up for each tumor type. *Events* is the number of death cases during follow up. *Median time* is given in days.

Tumor type	Non-significant	FDR < 0.05	Cases	Events	Median time
Kidney	12933	9166	881	227	N.A.
Uterus	16698	5400	596	125	3365
Liver	18521	3571	365	130	1694
Prostate	21458	638	496	10	N.A.
Colorectal	21641	455	602	128	2532

Continued on next page

Table S9. Survival analysis using Cox proportional regression showing the number of mRNAs with prognostic value accross the 13 cancer types. *Non-significant* column indicates the number of genes with FDR greater than 0.05. *Cases* represents the number patients at the beginning of follow-up for each tumor type. *Events* is the number of death cases during follow up. *Median time* is given in days.

Tumor type	Non-significant	FDR < 0.05	Cases	Events	Median time
Bladder	21674	424	407	178	1008
Thyroid	21721	374	504	16	N.A.
Stomach	21797	302	392	158	940
Lung	21922	177	998	395	1531
Breast	21998	101	1080	151	3941
HeadNeck	22020	78	501	217	1671
Bile	21952	0	36	18	1220
Esophagus	22099	0	184	77	784

Table S10. Differentially expressed mRNA genes with prognostic value across cancer types. *Good* indicates the Cox HR < 1. *Bad* represents Cox HR > 1. *N.P.* refers that the given gene is non-prognostic on this cancer type

	Bladder	Breast	Colorectal	HeadNeck	Kidney	Liver	Lung	Prostate	Stomach	Thyroid	Uterus
ENSG00000065328	N.P.	N.P.	N.P.	N.P.	Bad	Bad	N.P.	Bad	N.P.	N.P.	Bad
ENSG00000090889	N.P.	N.P.	N.P.	N.P.	Bad	Bad	N.P.	Bad	N.P.	N.P.	Bad
ENSG00000091651	N.P.	N.P.	N.P.	N.P.	Bad	Bad	N.P.	Bad	N.P.	N.P.	N.P.
ENSG00000092853	N.P.	N.P.	N.P.	N.P.	Bad	Bad	N.P.	Bad	N.P.	N.P.	N.P.
ENSG00000093009	N.P.	N.P.	N.P.	N.P.	Bad	Bad	N.P.	N.P.	N.P.	N.P.	N.P.
ENSG00000100162	N.P.	N.P.	N.P.	N.P.	Bad	Bad	N.P.	N.P.	N.P.	N.P.	N.P.
ENSG00000102384	N.P.	N.P.	N.P.	N.P.	Bad	Bad	N.P.	Bad	N.P.	N.P.	Bad
ENSG00000105011	N.P.	N.P.	N.P.	N.P.	Bad	Bad	N.P.	N.P.	N.P.	N.P.	N.P.
ENSG00000106268	N.P.	N.P.	N.P.	N.P.	Bad	Bad	N.P.	N.P.	N.P.	N.P.	N.P.
ENSG00000112984	N.P.	N.P.	N.P.	N.P.	Bad	Bad	N.P.	N.P.	N.P.	N.P.	Bad
ENSG00000115163	N.P.	N.P.	N.P.	N.P.	Bad	Bad	N.P.	N.P.	N.P.	N.P.	Bad
ENSG00000117650	N.P.	N.P.	N.P.	N.P.	Bad	Bad	N.P.	N.P.	N.P.	N.P.	N.P.
ENSG00000121152	N.P.	N.P.	N.P.	N.P.	Bad	Bad	N.P.	N.P.	N.P.	N.P.	Bad
ENSG00000126787	N.P.	N.P.	N.P.	N.P.	Bad	Bad	N.P.	N.P.	N.P.	N.P.	Bad
ENSG00000138180	N.P.	N.P.	N.P.	N.P.	Bad	Bad	N.P.	N.P.	N.P.	N.P.	N.P.
ENSG00000144554	N.P.	N.P.	N.P.	N.P.	Bad	Bad	N.P.	N.P.	N.P.	N.P.	N.P.
ENSG00000148773	N.P.	N.P.	N.P.	N.P.	Bad	Bad	N.P.	N.P.	N.P.	N.P.	N.P.
ENSG00000156970	N.P.	N.P.	N.P.	N.P.	Bad	Bad	N.P.	Bad	N.P.	N.P.	Bad
ENSG00000157456	N.P.	N.P.	N.P.	N.P.	Bad	Bad	N.P.	Bad	N.P.	N.P.	N.P.
ENSG00000162062	N.P.	N.P.	N.P.	N.P.	Bad	Bad	N.P.	N.P.	N.P.	N.P.	Bad
ENSG00000165304	N.P.	N.P.	N.P.	N.P.	Bad	Bad	N.P.	N.P.	N.P.	N.P.	N.P.
ENSG00000166508	N.P.	N.P.	N.P.	N.P.	Bad	N.P.	N.P.	N.P.	N.P.	N.P.	Bad
ENSG00000167513	N.P.	N.P.	N.P.	N.P.	Bad	Bad	N.P.	N.P.	N.P.	N.P.	N.P.
ENSG00000169679	N.P.	N.P.	N.P.	N.P.	Bad	Bad	N.P.	N.P.	N.P.	N.P.	Bad
ENSG00000186185	N.P.	N.P.	N.P.	N.P.	Bad	Bad	N.P.	Bad	N.P.	N.P.	Bad
ENSG00000189057	N.P.	N.P.	N.P.	N.P.	Bad	Bad	N.P.	N.P.	N.P.	N.P.	N.P.
ENSG00000076555	N.P.	N.P.	N.P.	N.P.	Good	N.P.	N.P.	N.P.	N.P.	N.P.	Bad
ENSG00000112425	N.P.	N.P.	N.P.	N.P.	Good	N.P.	N.P.	N.P.	N.P.	N.P.	Bad
ENSG00000130988	N.P.	N.P.	N.P.	N.P.	Good	Good	N.P.	N.P.	N.P.	N.P.	Bad
ENSG00000133800	N.P.	N.P.	N.P.	N.P.	N.P.	N.P.	N.P.	N.P.	N.P.	N.P.	Bad

Continued on next page

Table S10. Differentially expressed mRNA genes with prognostic value across cancer types. *Good* indicates the Cox HR < 1. *Bad* represents Cox HR > 1. *N.P.* refers that the given gene is non-prognostic on this cancer type

	Bladder	Breast	Colorectal	HeadNeck	Kidney	Liver	Lung	Prostate	Stomach	Thyroid	Uterus
ENSG00000138356	N.P.	N.P.	N.P.	N.P.	N.P.	N.P.	N.P.	N.P.	N.P.	N.P.	Bad
ENSG00000151623	N.P.	N.P.	N.P.	N.P.	Good	N.P.	N.P.	N.P.	N.P.	N.P.	N.P.
ENSG00000154330	N.P.	N.P.	N.P.	N.P.	Good	N.P.	N.P.	N.P.	N.P.	N.P.	N.P.
ENSG00000168546	N.P.	N.P.	N.P.	N.P.	Bad	N.P.	N.P.	N.P.	N.P.	N.P.	Bad
ENSG00000170271	N.P.	N.P.	N.P.	N.P.	Good	N.P.	N.P.	N.P.	N.P.	Bad	N.P.
ENSG00000185432	N.P.	N.P.	N.P.	N.P.	Good	N.P.	N.P.	N.P.	N.P.	N.P.	N.P.
ENSG00000198300	N.P.	N.P.	N.P.	N.P.	N.P.	N.P.	N.P.	N.P.	N.P.	Bad	N.P.

Table S11. Differentially expressed e-lncRNA genes with prognostic value across cancer types. *Good* indicates the Cox HR < 1. *Bad* represents Cox HR > 1. *N.P.* refers that the given gene is non-prognostic on this cancer type

	Bladder	Breast	Colorectal	HeadNeck	Kidney	Liver	Lung	Prostate	Stomach	Thyroid	Uterus
CATG00000107122	N.P.	N.P.	N.P.	N.P.	Bad	N.P.	N.P.	N.P.	N.P.	N.P.	N.P.
ENSG00000255958	N.P.	N.P.	N.P.	N.P.	N.P.	N.P.	N.P.	N.P.	Bad	N.P.	N.P.

Table S12. Differentially expressed dp-lncRNA genes with prognostic value across cancer types. *Good* indicates the Cox HR < 1. *Bad* represents Cox HR > 1. *N.P.* refers that the given gene is non-prognostic on this cancer type

	Bladder	Breast	Colorectal	Kidney	Liver	Lung	Prostate	Stomach	Thyroid	Uterus
CATG00000017193	N.P.	N.P.	N.P.	Bad	N.P.	N.P.	N.P.	N.P.	N.P.	N.P.
CATG00000020461	N.P.	N.P.	N.P.	Bad	N.P.	N.P.	N.P.	N.P.	N.P.	N.P.
CATG00000054098	N.P.	N.P.	N.P.	Bad	N.P.	N.P.	N.P.	N.P.	N.P.	N.P.
CATG00000087995	N.P.	N.P.	N.P.	N.P.	N.P.	N.P.	Bad	N.P.	N.P.	N.P.
CATG00000101363	N.P.	N.P.	N.P.	Bad	N.P.	N.P.	N.P.	N.P.	N.P.	Bad
ENSG00000235989	N.P.	N.P.	Bad	Bad	N.P.	N.P.	N.P.	N.P.	N.P.	Bad
ENSG00000247373	N.P.	N.P.	N.P.	Bad	N.P.	N.P.	N.P.	N.P.	N.P.	N.P.
ENSG00000255717	N.P.	N.P.	N.P.	Bad	Bad	N.P.	N.P.	N.P.	N.P.	Bad
ENSG00000257605	N.P.	N.P.	N.P.	Bad	N.P.	N.P.	N.P.	N.P.	N.P.	Bad
ENSG00000258384	N.P.	N.P.	N.P.	Bad	N.P.	N.P.	N.P.	N.P.	N.P.	N.P.
ENSG00000260442	N.P.	N.P.	N.P.	Bad	N.P.	N.P.	N.P.	N.P.	N.P.	N.P.
ENSG00000263412	N.P.	N.P.	N.P.	Bad	N.P.	N.P.	N.P.	N.P.	N.P.	Bad
ENSG00000270195	N.P.	N.P.	N.P.	Bad	N.P.	N.P.	N.P.	N.P.	N.P.	N.P.
ENSG00000272455	N.P.	N.P.	N.P.	Bad	N.P.	N.P.	N.P.	N.P.	N.P.	Bad
CATG00000105517	N.P.	N.P.	N.P.	N.P.	N.P.	N.P.	N.P.	N.P.	N.P.	Bad
ENSG00000226237	N.P.	N.P.	N.P.	Bad	N.P.	N.P.	N.P.	N.P.	N.P.	Bad
ENSG00000232160	N.P.	N.P.	N.P.	Good	N.P.	N.P.	N.P.	N.P.	N.P.	N.P.
ENSG00000234492	N.P.	N.P.	N.P.	Good	N.P.	N.P.	N.P.	N.P.	N.P.	N.P.
ENSG00000235652	N.P.	N.P.	N.P.	Good	N.P.	N.P.	N.P.	N.P.	N.P.	N.P.
ENSG00000248980	N.P.	N.P.	N.P.	Good	N.P.	N.P.	N.P.	N.P.	N.P.	N.P.
ENSG00000267414	N.P.	N.P.	N.P.	Good	N.P.	N.P.	N.P.	N.P.	N.P.	Bad
ENSG00000271849	N.P.	N.P.	N.P.	Good	N.P.	N.P.	N.P.	N.P.	N.P.	N.P.

Table S13. Differentially expressed ip-lncRNA genes with prognostic value across cancer types. *Good* indicates the Cox HR < 1. *Bad* represents Cox HR > 1. *N.P.* refers that the given gene is non-prognostic on this cancer type

	Bladder	Breast	Colorectal	HeadNeck	Kidney	Liver	Lung	Prostate	Stomach	Thyroid	Uterus
ENSG00000196756	N.P.	N.P.	N.P.	N.P.	Bad	N.P.	N.P.	Bad	N.P.	N.P.	Bad
ENSG00000260924	N.P.	N.P.	N.P.	N.P.	Bad	N.P.	N.P.	N.P.	N.P.	N.P.	N.P.
ENSG00000215386	N.P.	N.P.	N.P.	N.P.	N.P.	N.P.	N.P.	N.P.	N.P.	N.P.	Bad
ENSG00000263753	N.P.	N.P.	N.P.	N.P.	N.P.	N.P.	N.P.	N.P.	N.P.	Bad	Bad

Supplementary Figures

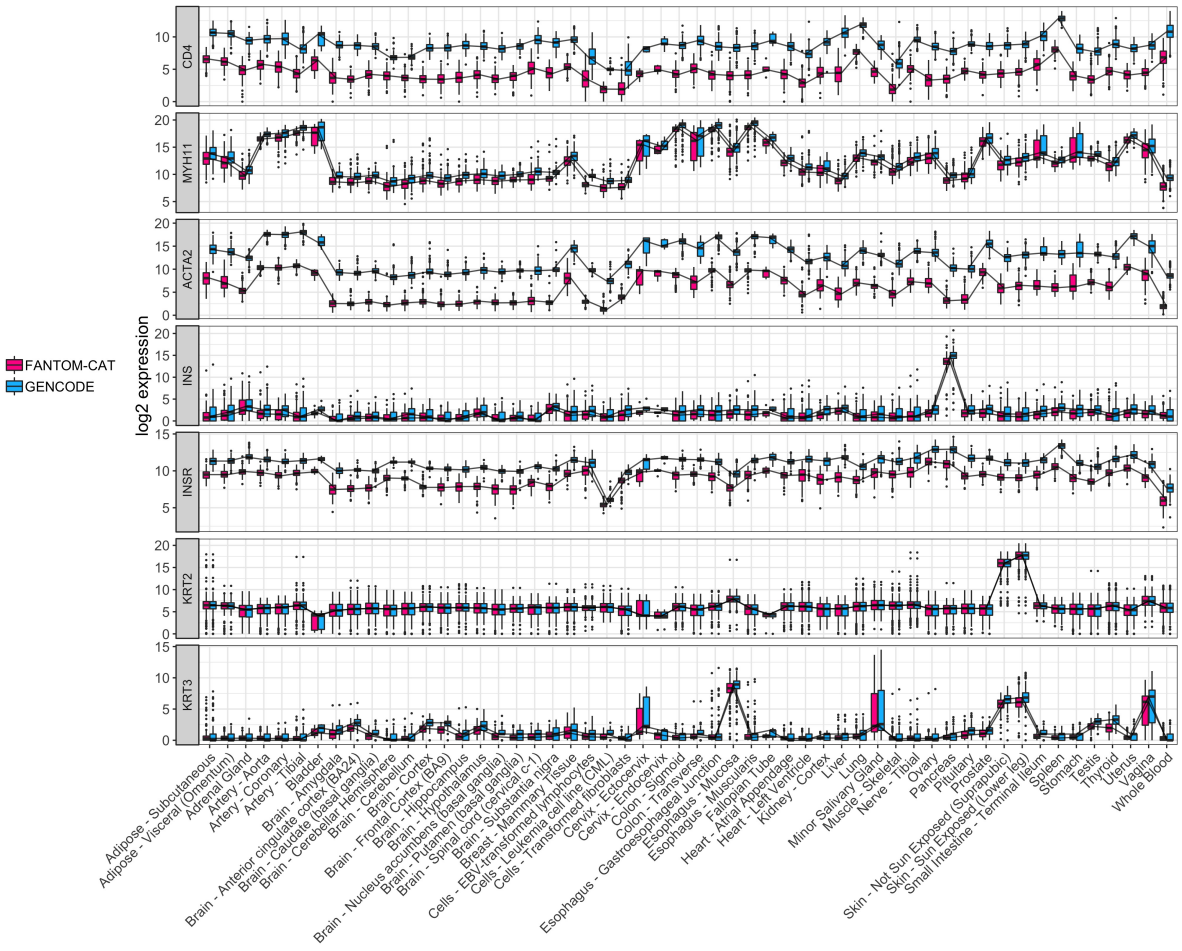

Figure S1. Tissue specific expression in GTEx. Log2 expression for tissue specific genes in GTEx data stratify by tissue type using `FC-R2` and GENCODE based quantification. Expression profiles are highly correlated and expressed consistently in the expected tissue types. *CD4* is most expressed in spleen, *MYH11* and *ACTA2* in tissues consisted of muscle cells, *INS* in pancreas and its receptor *INSR* globally, *KRT2* and *KRT3* in skin.

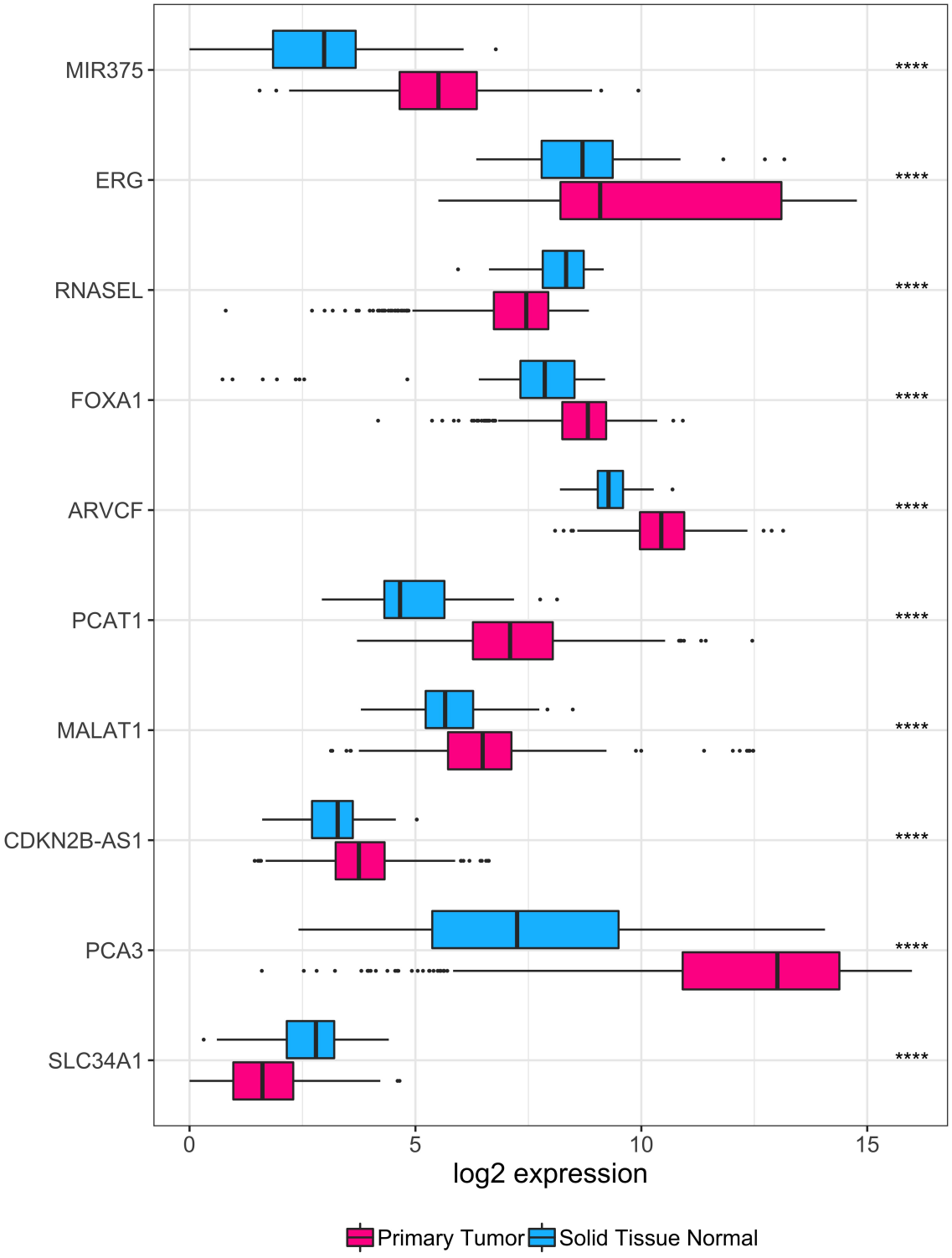

Figure S2. Expression levels for ncRNAs known to be involved in prostate cancer. Results are stratified by sample type. Stars indicate significance from the t.test: p-value is less than 10 raised to the negative number of stars ($p < 10^{-stars}$).

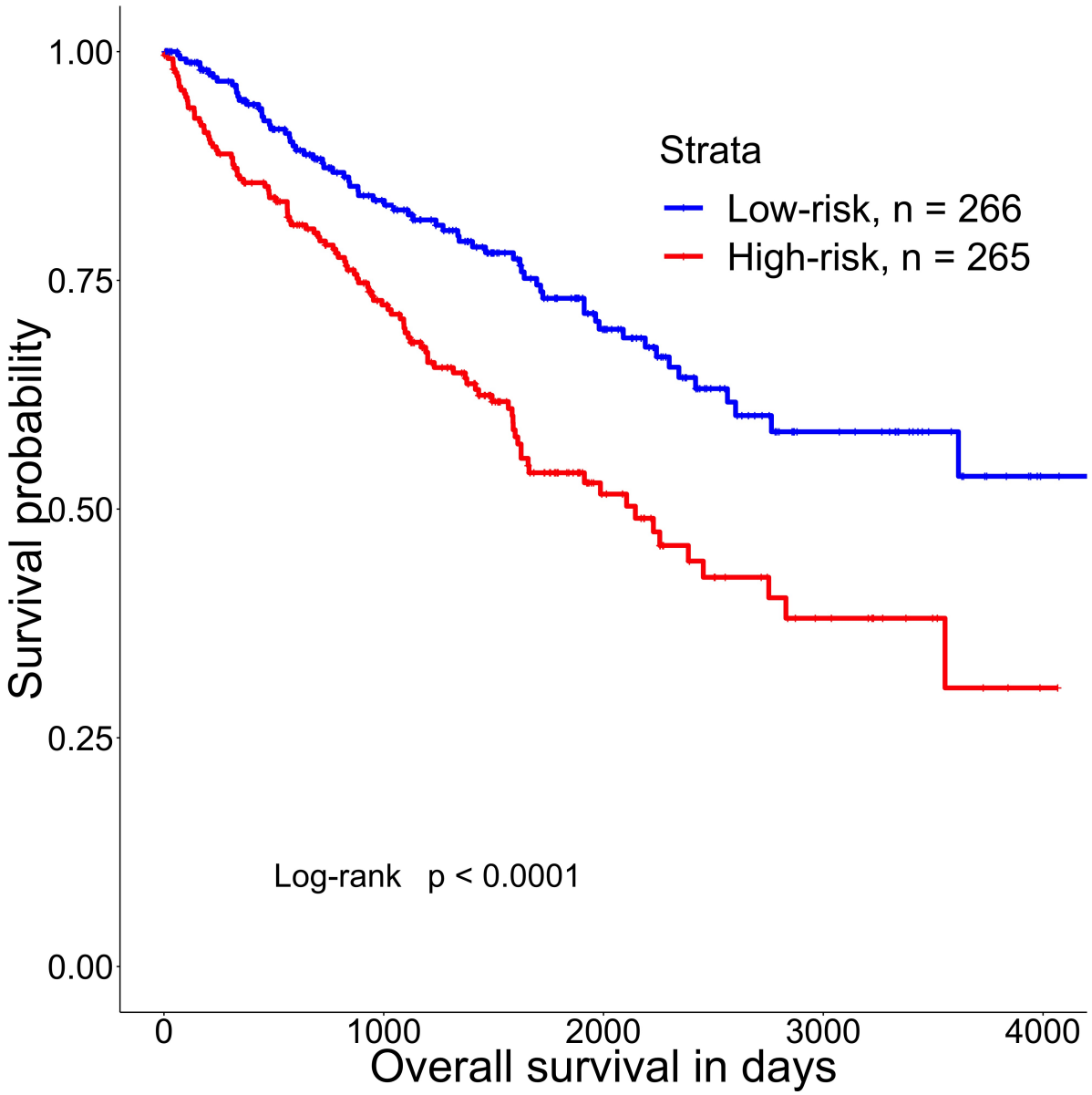

Figure S3. KM curve for enhancer 22. Kaplan-Meier survival curve depicting ENSG00000272666 (enhancer22 in Chen et al.[34]) groups split by median expression level for kidney clear cell renal cell carcinoma (KIRC) cases.

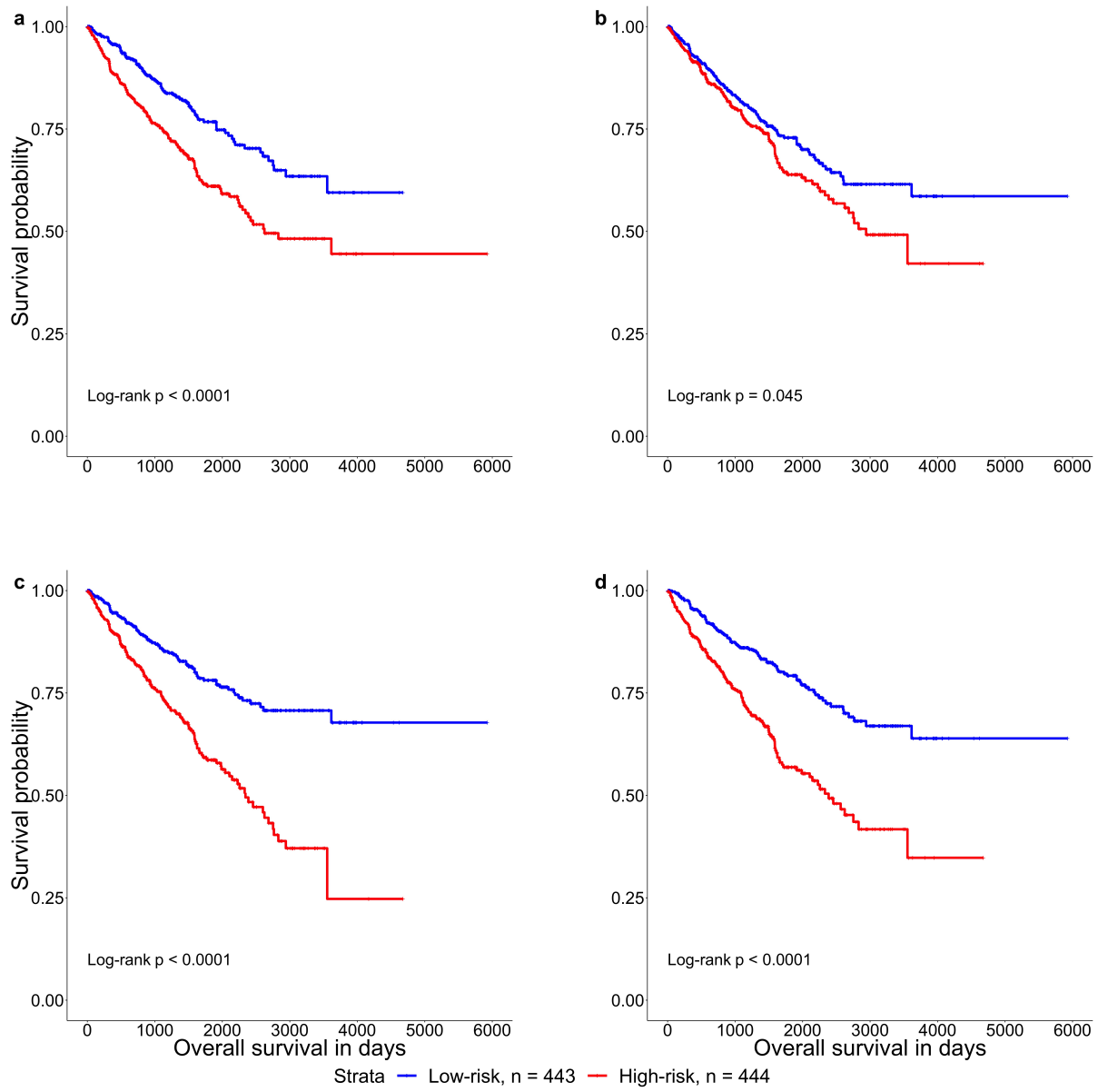

Figure S4. Kaplan-Meier survival curves depicting four selected differentially expressed genes holding predictive value in kidney cancers. a. mRNA gene ENSG00000065328 (*MCM10*), **b.** e-lncRNA gene CATG00000107122 unique to FANTOM-CAT, **c.** dp-lncRNA gene ENSG00000235989 (*MORC2-AS1*), **d.** ip-lncRNA gene ENSG00000196756 (*SNHG17*). Low- and high-risk groups were split by median expression level for each gene. Statistical significance were assessed using log-rank test.

1 Supplementary Methods

Data and pre-processing.

We obtained files containing coordinates of updated gene models of FANTOM-CAT permissive set from the ongoing FANTOM6 consortium. These files containing coordinates for 709,176 transcript models were imported into an R session and used to create a Genomic Range object with the GenomicRanges package[43] of all exons coordinates. Given the unstranded nature of recount2 we opted to remove overlapping exons belonging to different gene models to avoid over-quantification of these regions. To avoid losing strand information from annotation we first split exons coordinates by strand into two objects. We then used the `disjoin` function from Genomic Ranges package to generate disjoint segments in each strand, and then across strands. (Figure 5). Each segment coordinate was then assigned to the corresponding overlapping gene model. Segments that were assigned to more than one gene were discarded. The expression values for each segment was then quantified using *recount.bwtool*[44] (code at https://github.com/LieberInstitute/marchionni_projects). The resulting expression quantifications were processed to generate `RangedSummarizedExperiment` objects compatible with the *recount2* framework[7,42] (code at https://github.com/eddieimada/fcr2). The expression values for each segment was added to its respective gene model, resulting in the final object containing expression at gene level, which is distributed through the recount package and recount2 website.

Correlation with other studies.

Due to the decision of removing segments overlapping with more than one gene model, we further investigated if removal of these segments caused significant impact on expression levels. To achieve that we compared our GTEx counts tables to the published GTEx counts from *recount2*. The version 2 of the gene counts for the GTEx samples were downloaded from the recount website (https://jhubiostatistics.shinyapps.io/recount/). Next, we scaled each object to a 40M depth using the `scale_counts` function from recount package. After scalling, we obtained the intersection of the genes across both objects and computed the Pearson correlation for each gene. We further selected a few tissue markers to evaluate expression specificity across tissue types.

Expression specificity of tissue facets.

To analyze the expression level and specificity of each gene, we first scaled GTEx data to 40M depth using the `scale_counts` function from recount package. Genes were then stratified by RNA class (i.e. mRNA, e-lncRNA, dp-lncRNA, ip-lncRNA) and grouped by tissue type (n = 54 facets). The expression level for each gene was represented by the maximum transcripts per million (TPM) of all samples within a facet. The expression specificity was calculated as the empirical entropy of the mean expression values of each facet divide by the log2 of the number of facets, as follows

$$SPECIFICITY = 1 - (entropy(X)/log_2(N))$$

Where X is a vector of sample-average values for a given gene over all facets and N is the number of facets. The 99.99 percent confidence intervals for the expression of each category by facet were calculated based on TPM values. Genes with a TPM greater than 0.01 were considered expressed.

Identification of differentially expressed genes.

To perform differential gene expression analysis across cancer types we relied on TCGA data scaled to 40M depth using the `scale_counts` function from recount. We split each cancer dataset by RNA class (coding mRNA, intergenic promoter lncRNA, divergent promoter lncRNA and enhancer lncRNA) and removed all metastatic samples prior analysis. Each RNA class was treated independently.

The design matrices were created from a factor with two levels (Primary Tumor and Normal Tissue) by setting the normal tissues as the intercept. For each RNA class we removed genes with low expression (< 5 counts) in more than 1/3 of the total samples in each cancer type. After filtering, we normalized raw libraries sizes using method TMM with `calcNormFactors` from edgeR package. After normalization, we transformed the count data to log2-counts per million (logCPM), and estimated the mean-variance relationship to compute appropriate observation-level weights using `voom`.

Finally, we run surrogate variable analysis (SVA)[46] using the permutation procedure proposed by Buja and Eyuboglu[48] and added the first three most variable coefficients as covariates in our design matrix. A generalized linear model approach coupled with empirical Bayes standard errors[45] was then used for identifying differentially expressed genes between the samples. Correction for multiple testing was performed across RNA classes by merging the resulting p-values for each cancer type and applying the Benjamini-Hochberg method[47].

Prognostic enhancers analysis.

Univariate Cox proportional regression were performed in four RNA subtypes (22106 mRNAs, 17,404 e-lncRNAs, 6,204 dp-lncRNAs, and 1,948 ip-lncRNAs) available through `FC-R2` as predictors on each of the 13 TCGA cancer types with available survival follow-up. The gene expressions were obtained across cancer types on TCGA data scaled to 40M depth using the `scale_counts` function from recount. We split each cancer dataset by RNA class (coding mRNA, intergenic promoter lncRNA, divergent promoter lncRNA and enhancer lncRNA) using only primary tumor samples gene expression. Some patients had more than one sample, in such cases, the first sample was chosen for the gene expression levels. Each RNA class was treated independently. Survival analysis including Cox proportional regression was done using R survival package[49]. Survival data (follow-up and vital status) available in the phenotype data derived from *recount2 expressionSets* were used to create survival objects for each of the 13 cancer types. Cox proportional regression was done for each cancer type using one gene at a time (univariate regression) grouped on each of the four RNA categories surveyed. Genes were considered predictive if its FDR were equal or less than 0.05, using Benjamini-Hochberg[47] correction. The correction was done within a cancer type grouping all genes by RNA type (i.e. corrected for 22,106 genes if mRNA were surveyed). This procedure yielded the predictive genes list broken-down in the four RNA categories reported. For reporting differentially expressed genes (DEG) among all cancer

types that portrait predictive value, the DEG lists were surveyed on each of the significant prognostic genes lists generated during the univariate Cox analysis by cancer types and summary tables reporting the genes predictive potential as good (HR < 1), bad (HR > 1), and non-predictive (FDR > 0.05) were prepared. Kaplan-Meier curves were done using *survminer* R package[50]. Groups were defined using median gene expression level and significance were assessed by log-rank test (P-value $<$ 0.05).

Supplementary data from Chen et al.[34] containing enhancers position and prognostic potential were obtained from the original publication supplementary material. Liftover to hg38 genome assembly was performed to match `FC-R2` coordinates in order to compare both resources. Prognostic genes list provided in Chen's paper were compared to prognostic genes obtained using `FC-R2`.